PART I: Gyrokinetic Exact Fokker-Planck-Landau Collisions in Fusion Plasma Turbulence

D. R. Ernst[1]

featuring contributions from **Q. Pan,[1] P. Crandall,[4] D. Hatch[7]**

PART II: ITER-Relevant Turbulence Broadening of the Divertor Heat Flux Profile in DIII-D QH-Mode Pedestals

featuring contributions from **A. Bortolon,[2] C. S. Chang,[2] S. Ku,[2] F. Scotti,[3] H. Q. Wang,[5] Z. Yan,[6] Jie Chen,[4] C. Chrystal,[5] F. Glass,[5] M. Halfmoon,[7] S. Haskey,[2] D. Hatch,[7] R. Hood,[8] F. Khabanov,[6] F. Laggner,[9] C. Lasnier,[3] G. McKee,[6] T. L. Rhodes,[4] D. Truong,[8] J. Watkins[8]**

[1]MIT [2]PPPL [3]LLNL [4]UCLA [5]General Atomics
[6]Univ. Wisconsin [7]UT-Austin [8]Sandia Nat. Lab. [9]NC State Univ.

Presented (in person) at

PPPL Theory Seminar

MBG Auditorium, Princeton Plasma Physics Laboratory, May 16, 2024

Email: dernst@psfc.mit.edu

https://sites.mit.edu/darinernst/

MIT PSFC Plasma Science and Fusion Center

SciDAC MGK

How good are the model collision operators used in GK codes?

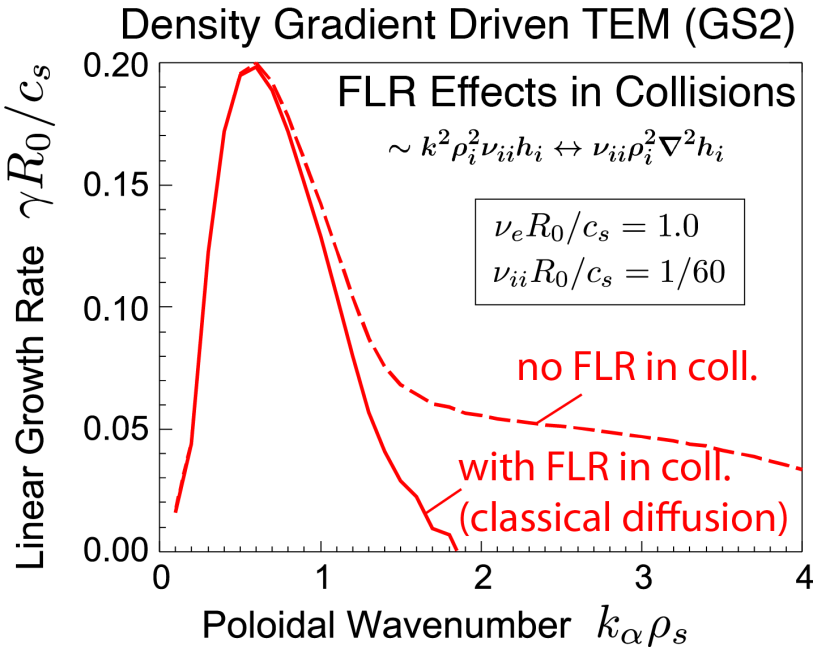

- Added classical diffusion + energy scattering to test particle operator [Ernst IAEA (2006)]

- **Model collision operators used in gyrokinetic codes**
  - Lorentz and variants, Kotschenreuther, Rewoldt, Tang (1995); Landau-like models (GENE and ORB5)
  - **Catto & Tsang (1977),** Xu & Rosenbluth (1991), Dimits & Cohen (1994), Lin (1995) [no H-theorem]
  - **Hirshman & Sigmar (1976)**, Abel et al. (2008): GK version, Catto & Ernst (2009), Sugama et al. (2009): Multi-species GK, Kolesnikov et al. (2010) [H-theorem]
- **Present *improved* GK models:**
  - **Sugama (2009)** (GENE, CGYRO, GKW); Sugama (2019); Frei et al. (2021, 2023) [moments]; Francisquez (2022), Kim (2022)

How good are the model collision operators used in GK codes?

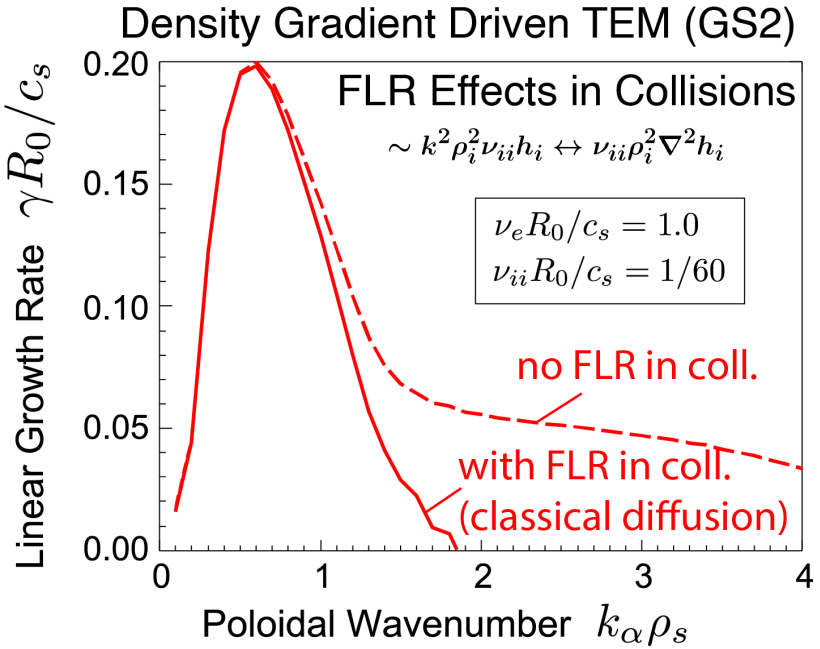

- **Important in turbulence:**
  - Energy diffusion
  - FLR effects
  - Impurities, isotopes
  - Conservation
  - H-theorem
- **Models conserve globally in velocity space, but miss local details**
  - Classical transport off 50%[1]
  - Neoclassical transport inaccurate[2-4]
- **Are model operators accurate for turbulence?**

[1]Catto & Ernst, PPCF (2009); [2]Wong & Chan, PPCF (2011); [3]Belli & Candy, PPCF (2012); [4]Landreman & Ernst, PPCF (2012)

We have formulated and implemented the gyrokinetic exact linearized Fokker–Planck operator

$$C_{ab}^{\mathrm{gk}}(h_a, h_b) = \left\langle e^{ik\cdot\rho_a}\, C_{ab}^{\mathrm{Linear}}\left(h_a e^{-ik\cdot\rho_a}, h_b e^{-ik\cdot\rho_b}\right)\right\rangle_{\underline{R}}$$

Gyro-average at fixed G.C. position **R**

- **Linearized operator is consistent with core and pedestal $\delta f \ll f_0$ orderings**
  - Linearized operator conserves particles, momentum, energy and satisfies H-theorem
  - In first order gyrokinetics, finite gyro-radius corrections do not affect conservation
  - Fundamental accuracy of Fokker-Planck-Landau operator ~ $1/\ln(\Lambda) \sim 10\%$
  - Nonlinear operator shown to be required near and outside separatrix (Hager 2016)
- **Formulated gyrokinetic exact linearized operator in two forms:**
  - In non-symmetric integro-differential "Rosenbluth" form (Li & Ernst, PRL 2011)
  - In conservative and symmetric Landau form (Pan & Ernst, PRE 2019)
- **Implemented GK Landau form in a gyrokinetic code (released in GENE-3.0)**
  - **Conserves particles, momentum, energy to machine precision, independent of resolution**
  - **Assess accuracy of GK collision models for the first time**

Rosenbluth form of gyrokinetic exact linearized Fokker–Planck collision operator formulated

- **Initial formulation in integro-differential "Rosenbluth" form[1]**

no FLR

FLR Test Particle Op.

$$\left(\frac{\partial h_a}{\partial t}\right)_c = C^{\mathrm{TP,DK}}_{\mathrm{PAS}}(h_a, f_{b0}) + C^{\mathrm{TP,DK}}_{\mathrm{ES}}(h_a, f_{b0}) + C^{\mathrm{TP,FLR}}(h_a, f_{b0})$$

Field operator

$$+ \boxed{\nu_a \frac{2}{\sqrt{\pi}} \left\{ \frac{2m_a}{m_b} h_b J_0 \left(\frac{k v_\perp}{\Omega_a} \left[1 - \frac{\Omega_a}{\Omega_b} \right] \right) + \int d^2 v' h'_b(v', \xi') I(v, \xi, v', \xi', k) \right\} e^{-v^2/v^2_{Ta}}}$$

- **Simple form for test particle FLR correction (most important collisional FLR term)[2]**

$$(\xi = v_\parallel / v) \qquad C^{\mathrm{TP,FLR}} = -[\nu_D(1+\xi^2) + \nu_\parallel(1-\xi^2)] \left(\frac{kv}{2\Omega_a} \right)^2 h_a$$

"Classical diffusion"
$\sim k^2 \rho_i^2 \nu_{ii} h_i \leftrightarrow \nu_{ii} \rho_i^2 \nabla^2 h_i$

- **Field operator involves Bessel functions and 2D velocity integral over field (b)**
  - When $k = 0$, $I = I_0$ can be expressed in terms of complete elliptic integrals E, K
  - For $k \neq 0$, $I = \sum_n c_n J_n(k v_\perp / \Omega_a) J_n(k v'_\perp / \Omega_b)$ (Bessel functions)

[1]Li and Ernst, PRL (2011).
[2]Catto and Tsang, PF B (1978).

Conservative Landau form of gyrokinetic exact operator formulated

Several slides adapted from Q. Pan APS invited talk (2019)

- **Linearized operator: test- and field-particle contributions, and FLR effects**

$$C_{ab}^{\mathrm{gk}}\left(h_a, h_b\right)/\Gamma_{ab} = -\nabla\cdot\left(\underline{J}_{ab}^{\mathrm{test}} + \underline{J}_{ab}^{\mathrm{field}}\right) + (\text{add'l FLR terms})$$

$$\underline{J}_{ab}^{\mathrm{test}} = \int d^2v' \left(\frac{h_a}{m_b}\underline{\underline{I}}_{E}^{\mathrm{test}}\cdot\nabla' f'_{b0} - \frac{f'_{b0}}{m_a}\underline{\underline{I}}_{D}^{\mathrm{test}}\cdot\nabla h_a\right)$$

$$\underline{J}_{ab}^{\mathrm{field}} = \int d^2v' \left(\frac{f_{a0}}{m_b}\underline{\underline{I}}_{E}^{\mathrm{field}}\cdot\nabla' h'_b - \frac{h'_b}{m_a}\underline{\underline{I}}_{D}^{\mathrm{field}}\cdot\nabla f_{a0}\right)$$

- **FLR terms and entries of 2 × 2 tensors $I_{E,D}^{\mathrm{test,field}}$ are written as gyrophase integrals**

$$I_{\mu\nu} = \oint\frac{d\phi}{2\pi}\oint\frac{d\phi'}{2\pi} g_1\left(\phi\right) g_2\left(\phi'\right) g_3\left(k\rho'\sin\phi' - k\rho\sin\phi\right) U_{\mu\nu}$$

$$g_j \in \{1, \sin(), \cos()\};\ U_{\mu\nu} \equiv \underline{e}_\mu\cdot\frac{u^2\underline{\underline{I}} - \underline{u}\,\underline{u}}{u^3}\cdot\underline{e}_\nu;\ \underline{u} = \underline{v} - \underline{v}';\ \mu,\nu\in\{\|,\perp,\phi\}$$

Pan & Ernst, PRE (2019)

Gyrokinetic exact operator vs. models

- **Construct gyrokinetic model operators:**
  - Take exact linearized test-particle terms (PA scattering + energy diffusion)
  - Expand field-particle terms in spherical harmonics in Ω and Sonine polynomials in v, and cut off high-order harmonics and moments (Hirshman & Sigmar, 1976).
  - Preserve conservation and H theorem by renormalizing coefficients
  - Gyrokinetic transformation (Catto & Tsang, 1977; Abel et al., 2008)

C (h) = exact test-particle terms + model field-particle terms + FLR effects

- **Model field-particle terms involve moments, while exact field-particle terms are 2D integrals of field-particle distribution and gyrophase integrals.**

Numerical Implementation and Verification

Finite-volume discretization of gyrokinetic exact operator

$$\frac{\partial h_a}{\partial t} = -\nabla \cdot \left(\underline{J}_{ab}^{\text{test}} + \underline{J}_{ab}^{\text{field}} \right) + (\text{add'l FLR terms}), \quad \underline{J}_{ab}^{\text{field}} \sim \int d^2 v' \underline{\underline{I}} \cdot \nabla' h_b'$$

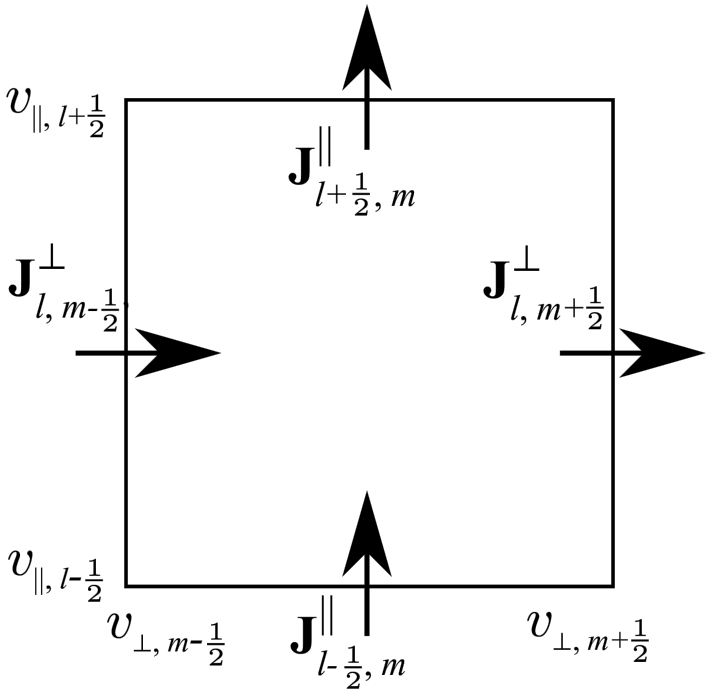

- **As in Yoon et al. (2014) and Hager et al. (2016) for nonlinear drift-kinetic Landau operator:**
  - divergence → finite-volume difference
  - integrations → summations
  - gradients → centered differencing
  - conserve particles, momentum, energy
- **FLR effects: elliptic integrals → gyrophase integrals**

Pre-compute gyrophase integrals ($I_{\mu v}$) using rectangular rule

- **Why rectangular integration in gyrophase ϕ and ϕ'?**
  - Periodic and smooth integrands → spectral convergence
  - Fixed grids ensure cancellation of numerical errors due to symmetry
- **Test-particle coeffs: numerical Landau form matches analytical Rosenbluth form**

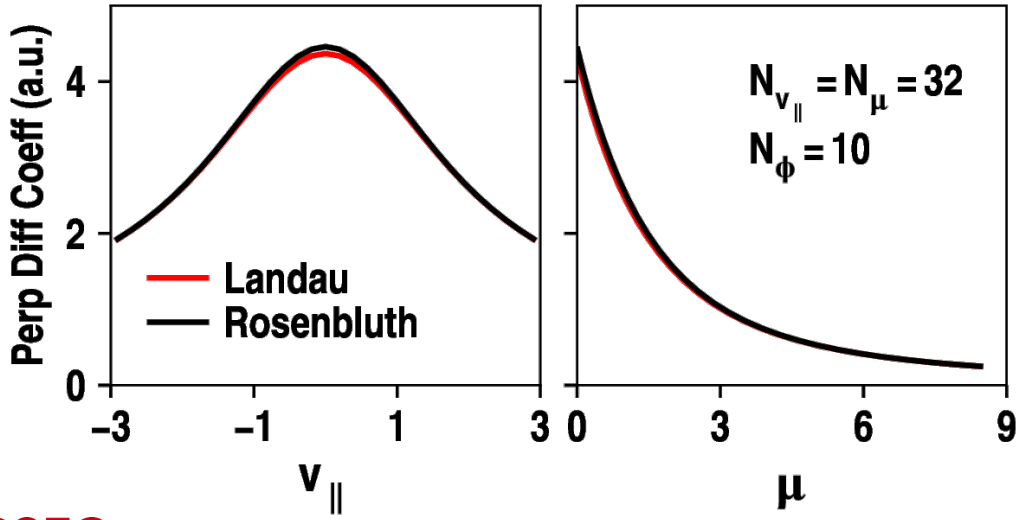

$$\underline{J}_{ab}^{\text{test}} \sim \int d^2v' f'_{b0} \underline{\underline{I}}_D^{\text{test}} \cdot \nabla h_a$$

Pan, Ernst, Crandall PoP (2020)

Number of gyrophase gridpoints required increases linearly with wavenumber

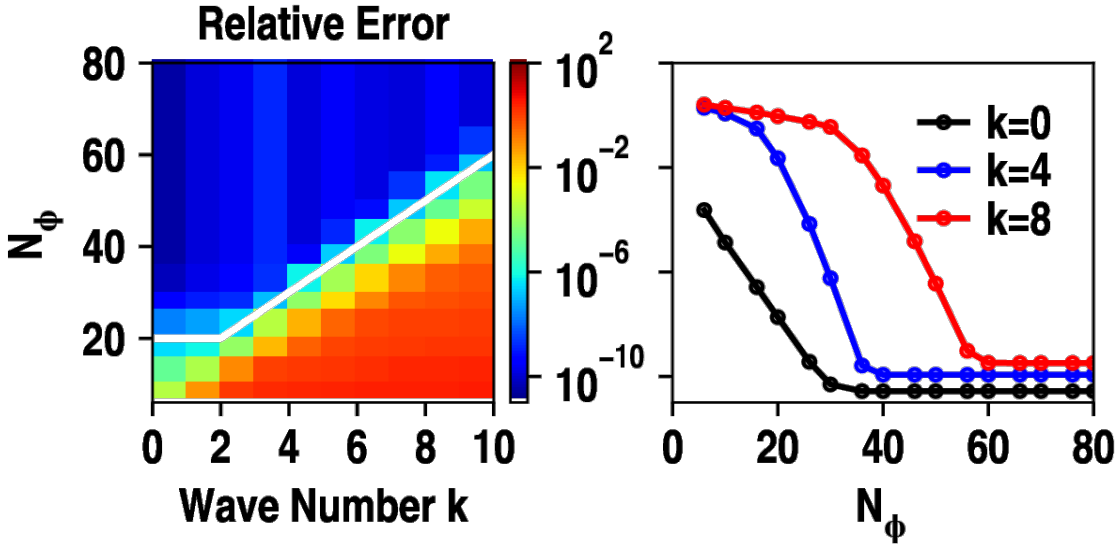

$$\underline{J}_{ab}^{\text{field}} \sim \int d^2v' f_{a0} \underline{\underline{I}}_{E}^{\text{field}} \cdot \nabla' h_b'$$

- Field-particle coeffs depend on k, use $N_\phi \approx \max(5k + 10, 20)$ to maintain same error (but precomputed anyway)
- Fixing k, error decays exponentially as N_ϕ increases

Gyrokinetic exact Landau form implemented in GENE preserves conservation (to machine precision) and H-theorem

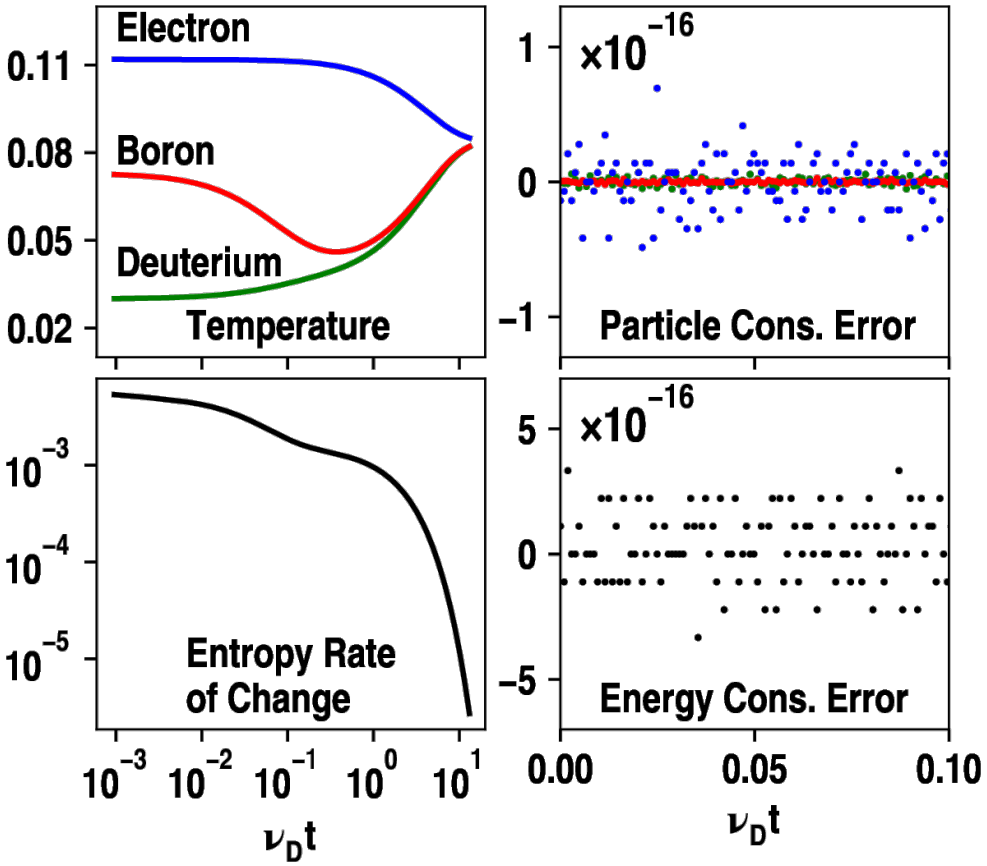

- Ion–electron equilibrate slower than between ions
- Entropy increases when resolution is sufficient. Here $N_{v||} = N_\mu = 32$.
- Conserved even if $N_{v||} = N_\mu = 4$.

Compare Gyrokinetic Exact Operator with Models

Sugama model overestimates neoclassical ion transport by 15-25%

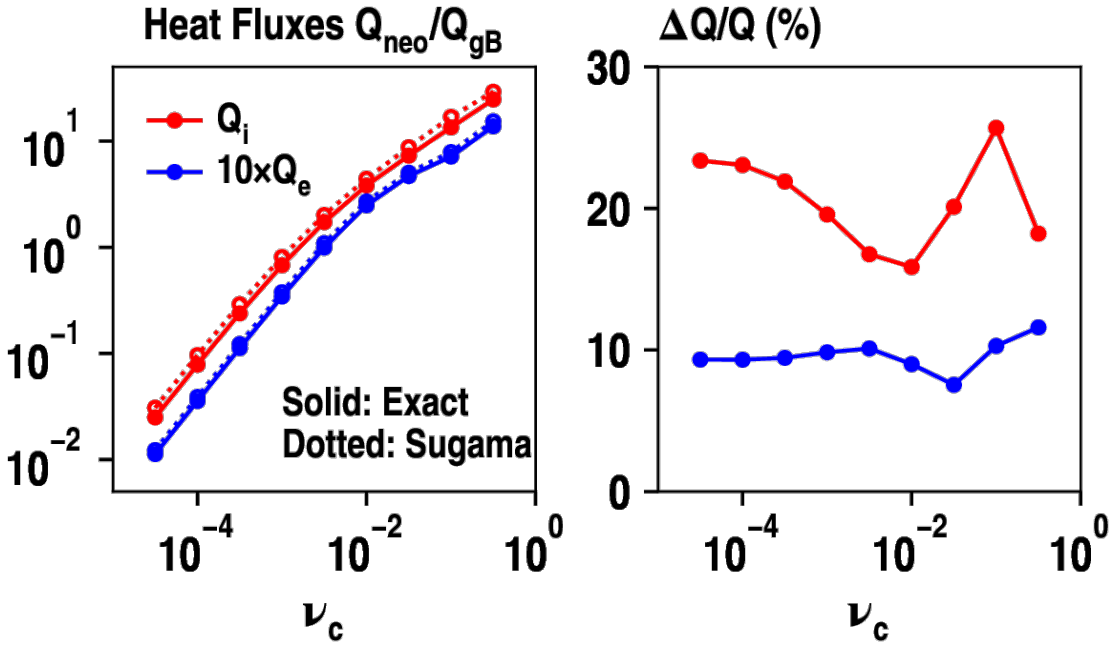

- Belli & Candy, PPCF (2012)
  Crandall et al. (2018)
- $Q_i \sim 20Q_e$
- Sugama model overestimates Q_e by 10% from banana to Pfirsch–Schlüter regime

- **Exact Linearized Fokker-Planck operator:**
  - Wong & Chan PPCF (2011); Landreman & Ernst PPCF (2012), Belli & Candy PPCF (2012)
- **Exact Nonlinear Fokker-Planck operator (needed near and outside separatrix):**
  - Sauter et al, CPP (1994); Yoon & Chang (2014), Dorf et al. (2014), Hager et al. (2016)

Pan, Ernst, Crandall PoP (2020)

Sugama model appears to be accurate for Density Gradient Driven TEM

$(\eta_e = 0)$

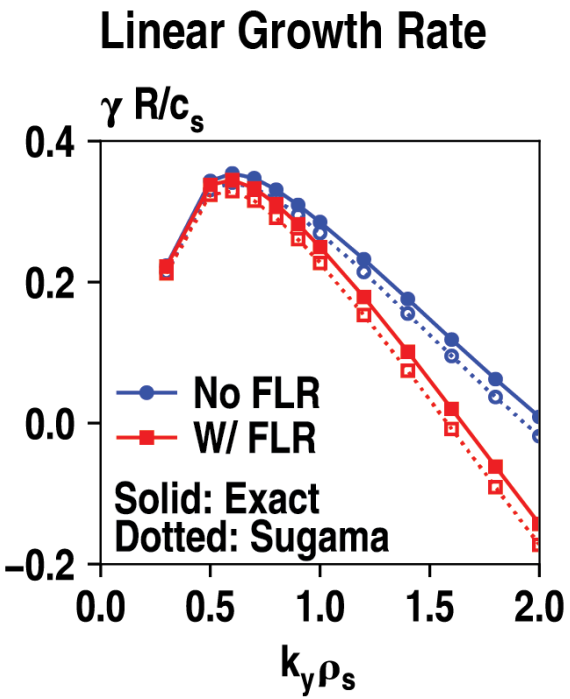

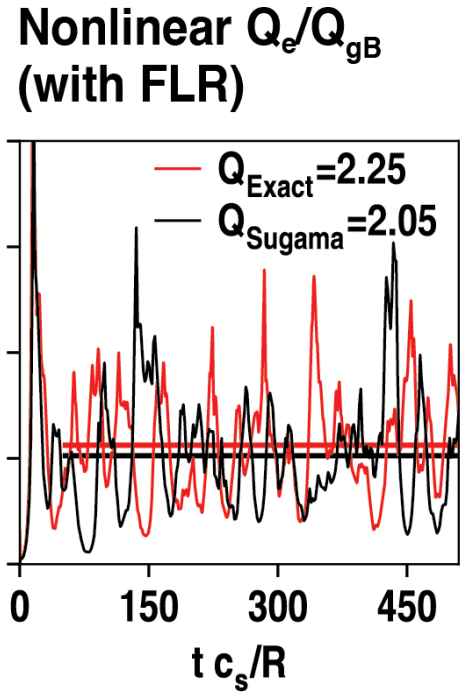

- **Sugama model captures growth rate spectrum and its reduction by FLR effects**
  - Dominant contribution is from test-particle terms
- **Sugama model also matches nonlinear TEM electron heat fluxes within 10%**

Pan, Ernst, Crandall, PoP (2019)

But Sugama model less accurate for TEM as η_e (= d ln Te/d ln n) and collisionality increase

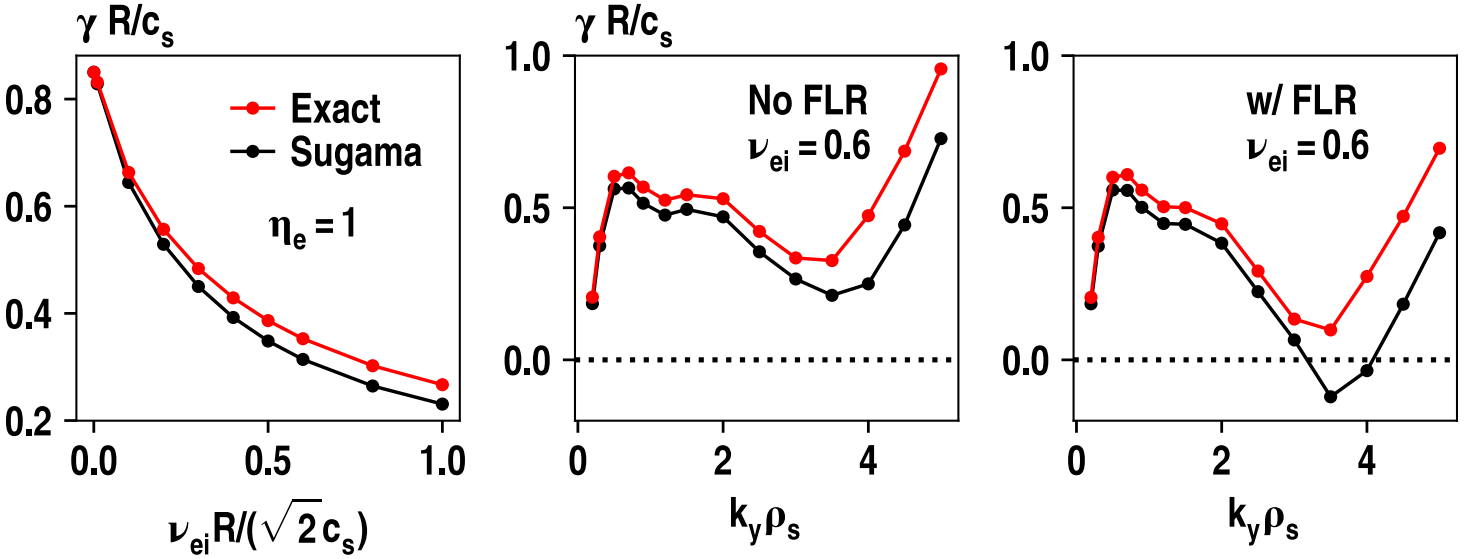

- At $\eta_e = 1$ and $\nu_{ei} R/v_{Ti} = 1$, peak growth rate using exact operator is 15% larger than model.
- Unstable mode extends from TEM to ETG using exact operator, but model finds false stable region at $k_y \rho_s = 3.2 - 4.0$.

Differences between Sugama and exact in linear TEM growth rates are largest for $\eta_e = L_{ne}/L_{Te} \sim 1.25$

- **Correction increases with collision frequency**
- **Correction peaks at $\eta_e \sim 1.25$**
- **For $\eta_e > 1.5$, correction decreases**
  - Growth rate increases, causing ν_{ei}/γ to decrease
  - Collisions become less important

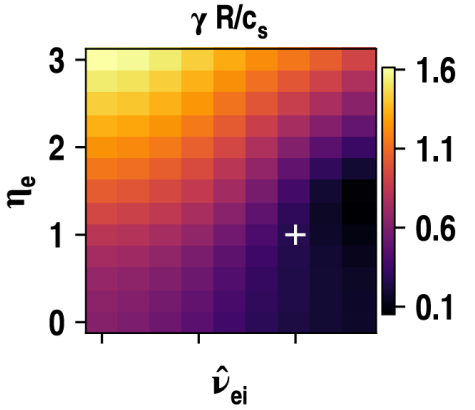

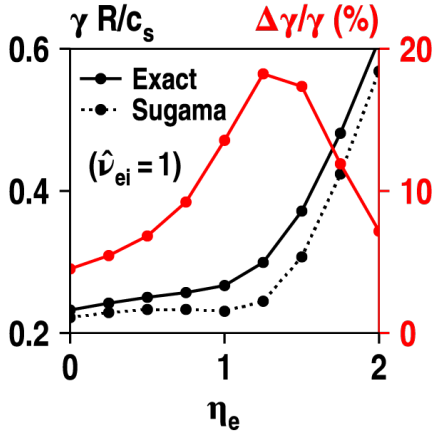

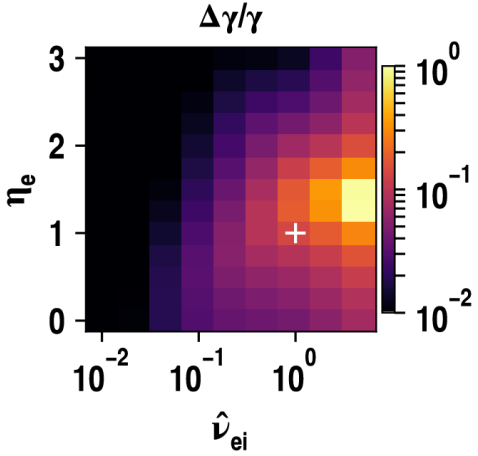

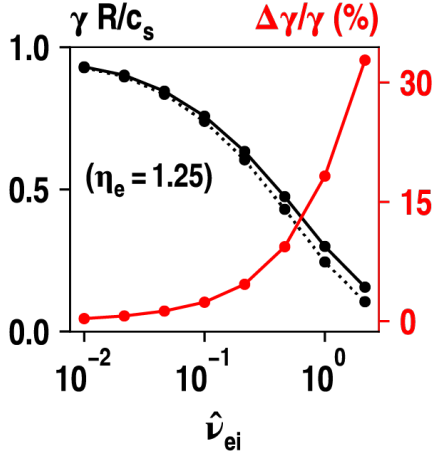

Pan, Ernst, Hatch, PRE Lett. (2021)

Exact field operator terms are most important for temperature gradient driven instabilities – why?

- Simplest TEM dispersion relation
- Electron temperature gradient η_e enters with energy weighting, driving distortions at higher energies in the distribution

energy

$$0 = 1 - \frac{\omega_{*e}}{\omega} F\left(\eta_i, k_\theta \rho_i\right) + \frac{\eta_i \omega_{*e} \omega_{De}}{\omega^2} + \frac{n_T}{n} \frac{2}{\sqrt{\pi}} \int_0^\infty dx \sqrt{x} e^{-x} \frac{\omega - \omega_{*e}\left[1 + \eta_e (x - 3/2)\right]}{\omega - \bar{\omega}_{De}(x)} \Bigg|_{x = E/T}$$

- Recall that model operators truncate a modified Laguerre energy expansion of the exact field operator terms. These truncated higher energy moments matter.

Nonlinear TEM Simulations show 68% larger flux from exact operator

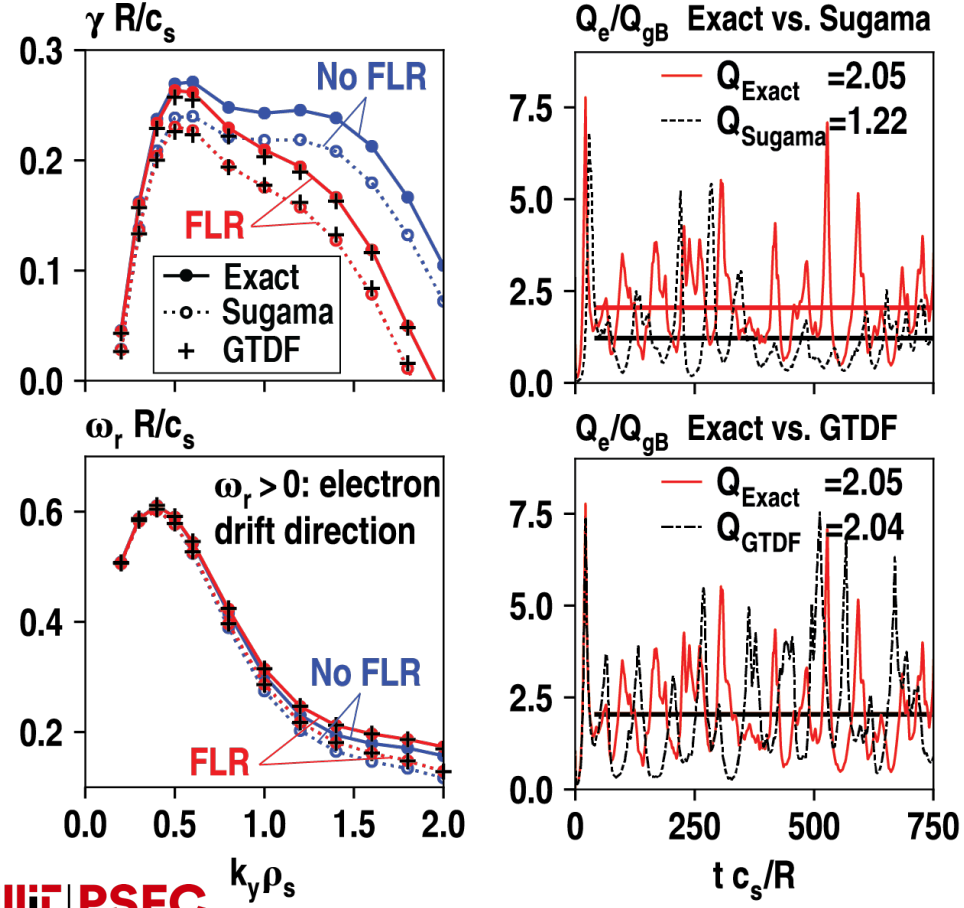

- $\eta_e = 1, \quad \hat{\nu}_{ei} = 1$ TEM
- Turning off FLR corrections in field operator, while retaining classical diffusion in test operator does not change results
- This suggests a reduced model:

  GTDF = "Gyrokinetic Test particle, Drift Kinetic Field particle operator"

Pan, Ernst, Hatch, PRE Lett. (2021)

Exact operator also shows corrections for microtearing modes in the JET pedestal with ITER-like wall

- **MTMs again driven by the electron temperature gradient**

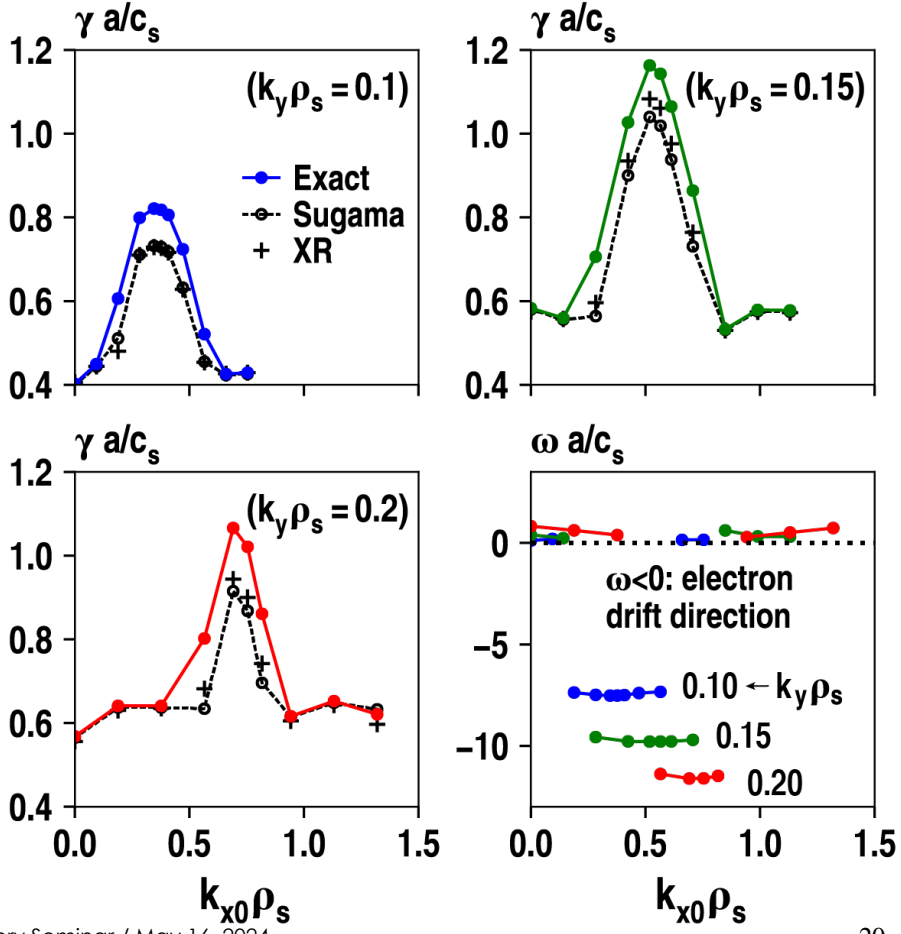

Pan, Ernst, Hatch, PRE Lett. (2021)

Exact operator displays weaker zonal flow damping than Sugama model

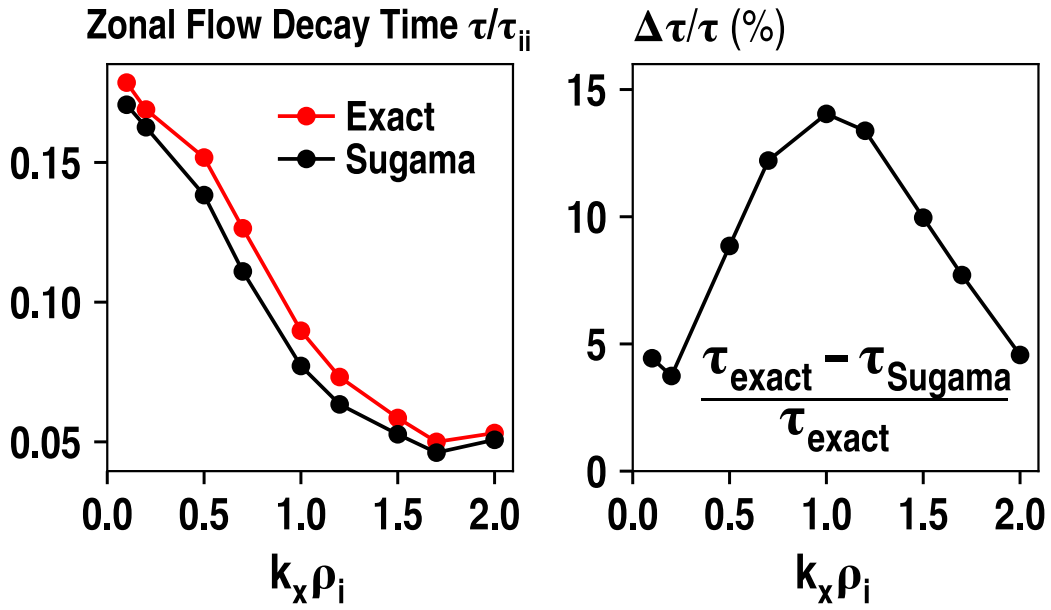

- Parameters as in Hinton & Rosenbluth, PPCF (1998).
- Decay times using exact operator are up to 15% longer (at $k_x\rho_i \sim 1$) than model.

Pan, Ernst, Crandall PoP (2020)

Summary of key results

- Exact GK linearized Landau operator produces up to 68% larger electron heat fluxes from TEM turbulence than the Sugama (2009) model
- Corrections are maximum for $\eta_e \sim 1.25$ for typical parameters
- Exact operator also shows weaker zonal flow damping

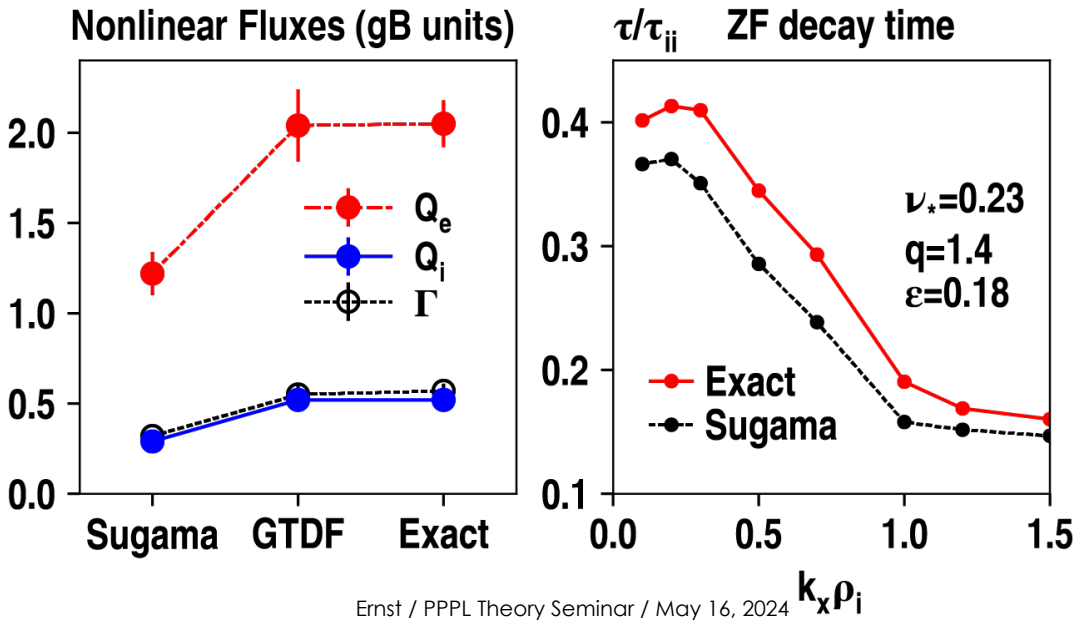

Conclusions

- **Conservative and symmetric formulation of gyrokinetic exact Landau operator enables numerical methods (finite-volume or spectral) to preserve conservation.**
- **GK exact operator has been correctly implemented in GENE: conservation, H theorem, test-particle equivalence to Rosenbluth form, neoclassical benchmarks**
- **Model operators have been tested against the GK exact operator for the first time (using the same finite-volume method). Exact field operator yields important corrections:**
  - Sugama model overestimates neoclassical ion heat flux by 15-25%, zonal flow decay rate by 15%.
  - FLR effects suppress TEM growth rates and reduce nonlinear fluxes by ~20%.
  - Sugama model least accurate for TEM growth rates for $\boldsymbol{\eta_e \sim 1.25}$ and larger $\hat{\boldsymbol{\nu}}_{\boldsymbol{ei}}$, with 68% larger electron heat flux for $\eta_e = 1$ and $\hat{\nu}_{ei} = 1$
- **Turning off FLR corrections in field term appears to have little effect on fluxes, motivating "GTDF" model with classical diffusion term as only FLR correction to DK operator**
- **Adding the test particle classical diffusion term $\sim k^2\rho_i^2\nu_{ii}$ ↔ $\nu_{ii}\nabla^2$ to the drift-kinetic operator will capture the main FLR effects in the gyrokinetic exact collision operator**

Discussion and ongoing work

- **Continuing to explore implications of GK exact operator in physically-relevant regimes. Parameter scans.**
- **2D velocity integrals in field-particle terms → MPI allgather, $\mathcal{O}(\mathcal{N}_v^2)$**
  - Optimizing communication load and time-stepping.
- **Spectral method in velocity** (Landreman & Ernst, JCP, 2013; PPCF 2012)
  - Non-classical polynomial co-location points with exact FP DK operator
  - PERFECT pedestal neoclassical code achieved same accuracy with 4 polynomials in speed compared with 100 – 200 modified Laguerres in other codes

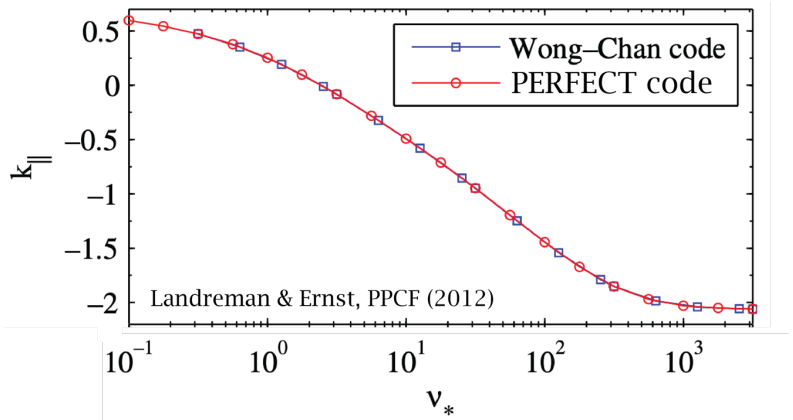

References

[1] B. Li and D. R. Ernst, Phys. Rev. Lett. **106**(19) 195002 (2011). https://doi.org/10.1103/PhysRevLett.106.195002

[2] Q. Pan and D. R. Ernst, Phys. Rev. E **99**, 023201 (2019). https://doi.org/10.1103/PhysRevE.99.023201

[3] Q. Pan, D. R. Ernst, and D. Hatch, Phys. Rev. E Lett. **103**, L051202 (2021). https://doi.org/10.1103/PhysRevE.103.L051202

[4] Q. Pan, D. R. Ernst and P. Crandall, Physics of Plasmas **27**, 042307 (2020). https://doi.org/10.1063/1.5143374

[5] M. Landreman and D. R. Ernst, J. Comput. Phys. **243**, 130 (2013). https://doi.org/10.1016/j.jcp.2013.02.041

[6] D. R. Ernst, A. Bortolon, C. S. Chang, S. Ku et al., Phys. Rev. Lett. (2024) accepted for publication. https://arxiv.org/abs/2403.00185

[7] M. Landreman and D. R. Ernst, Plasma Phys. Control. Fusion **54** 115006 (2012). http://dx.doi.org/10.1088/0741-3335/54/11/115006

Other references made can be found in the reference lists of the articles above.

Backup Slides

GENE (finite-volume) agrees with CGYRO (spectral) for Sugama model

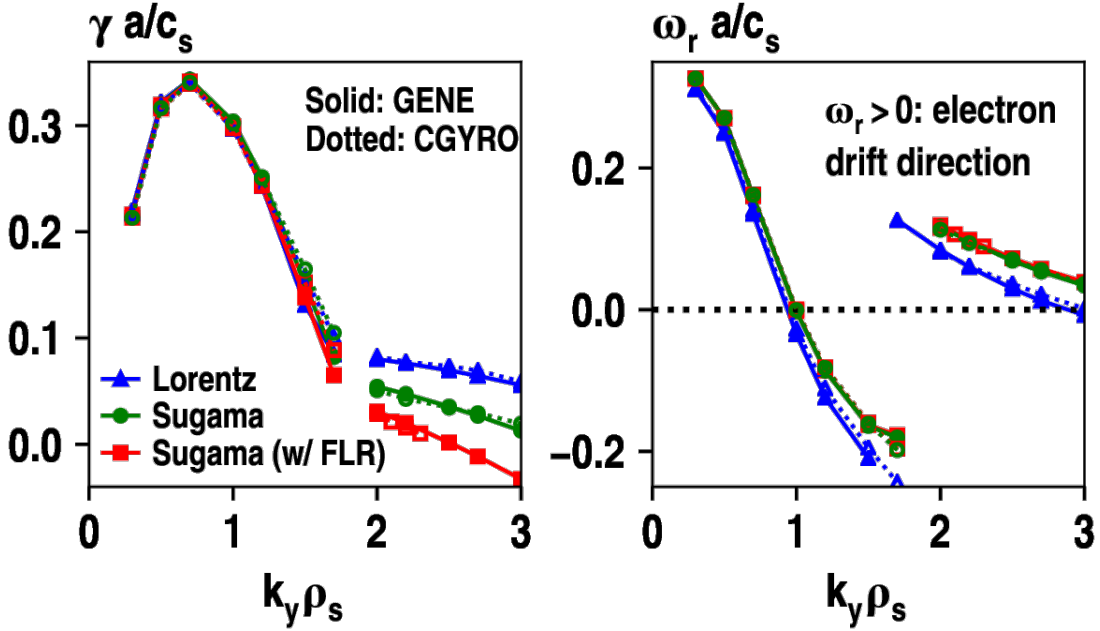

- Linear scans of density gradient TEM (DGTEM)
- CGYRO data from Belli & Candy, PPCF (2017)
- Sugama operator implemented in GENE by Crandall et al. (2018)

PART I: Gyrokinetic Exact Fokker-Planck-Landau Collisions in Fusion Plasma Turbulence

D. R. Ernst[1]

featuring contributions from **Q. Pan,[1] P. Crandall,[4] D. Hatch[7]**

PART II: ITER-Relevant Turbulence Broadening of the Divertor Heat Flux Profile in DIII-D QH-Mode Pedestals

featuring contributions from **A. Bortolon,[2] C. S. Chang,[2] S. Ku,[2] F. Scotti,[3] H. Q. Wang,[5] Z. Yan,[6] Jie Chen,[4] C. Chrystal,[5] F. Glass,[5] M. Halfmoon,[7] S. Haskey,[2] D. Hatch,[7] R. Hood,[8] F. Khabanov,[6] F. Laggner,[9] C. Lasnier,[3] G. McKee,[6] T. L. Rhodes,[4] D. Truong,[8] J. Watkins[8]**

[1]MIT [2]PPPL [3]LLNL [4]UCLA [5]General Atomics
[6]Univ. Wisconsin [7]UT-Austin [8]Sandia Nat. Lab. [9]NC State Univ.

Presented (in person) at

PPPL Theory Seminar

MBG Auditorium, Princeton Plasma Physics Laboratory, May 16, 2024

Email: dernst@psfc.mit.edu

https://sites.mit.edu/darinernst/

MIT PSFC Plasma Science and Fusion Center

SciDAC MGK

Turbulence Broadening of Divertor Heat Flux Width λ_q Demonstrated in Turbulence Limited QH-Mode Pedestals using Direct Measurements

Eich function fitted to divertor Langmuir probe $q_{||}$ profiles [T. Eich NF 2013]

$$q_{||}(\bar{s}) = \frac{q_0}{2} \exp\left[\left(\frac{S}{2\lambda_q}\right)^2 - \frac{\bar{s}}{\lambda_q f_x}\right] \operatorname{erfc}\left(\frac{S}{2\lambda_q} - \frac{\bar{s}}{S f_x}\right) + q_{\mathrm{BG}}$$

$$\bar{s} = s - s_0 = (R_{\mathrm{mid}} - R_{\mathrm{sep}}) f_x$$

$f_x = 5.3$ **flux area expansion factor**

$$\lambda_{\mathrm{int}} = \frac{\int [q_{||}(s) - q_{\mathrm{BG}}] ds}{q_{||0}} \approx \lambda_q + 1.64\, S$$

Integral heat flux width at divertor

- **Both λ_q and S increase with $\tilde{n}/n$**
- **I_p scan shows no trend with B_p – does not follow ITPA scaling**

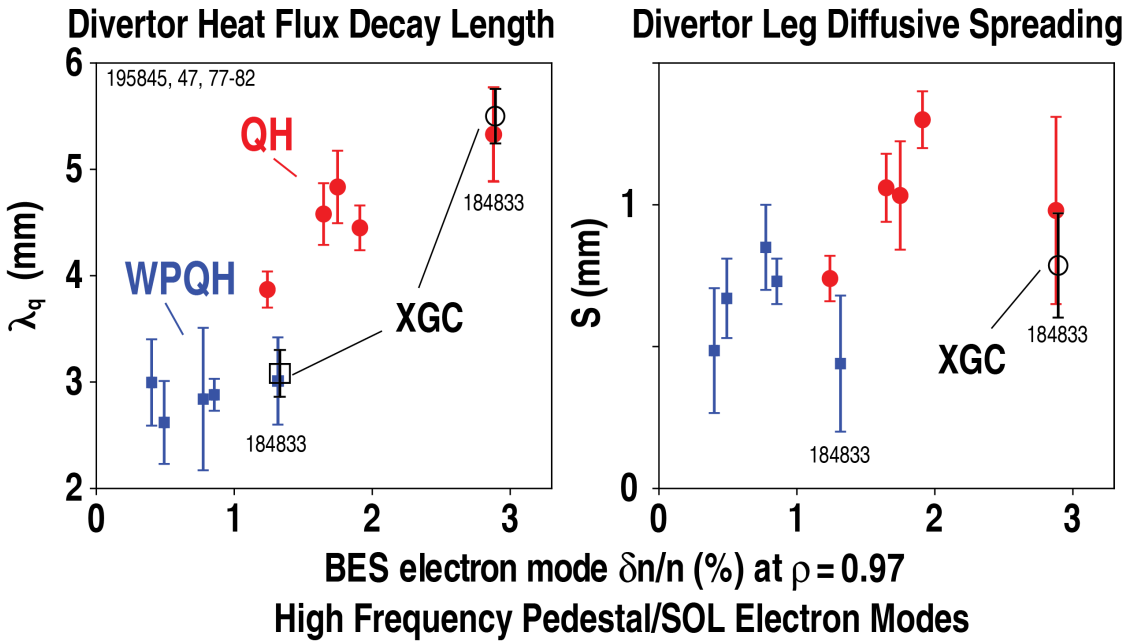

XGC simulations by S. Ku

Ernst et al., arXiv (2024), PRL accepted (2024).

Wide Pedestal QH-Mode is an example of a Turbulence-Limited Pedestal where *Reduced* Pedestal ExB Shear *Improves* Confinement

- **QH-Mode is obtained after a fresh boronization**
  - Reduced L-Mode density increases temperature, reducing collisionality
  - Low collisionality increases pedestal bootstrap current
- **QH-Mode operates close to current-driven peeling mode stability boundary, limited by**
  - Low-n EHO, *or*
  - Broadband turbulence
- **QH-Mode pedestal width Δ follows EPED scaling: $\Delta \sim \beta_p^{0.5}$**

- **QH-Mode transitions to Wide Pedestal QH-Mode[1,2] upon reducing NBI torque below 2 Nm**
  - Pedestal Pressure ⇧ 60%; Width ⇧ 65%; τ_E ⇧ 40% (≤1.6)
  - Turbulence broadens pedestal, allowing KBM-PBM stable access to higher β_p
  - Sustained with up to 77% ECH power[3] without confinement degradation, zero net NBI torque[4]

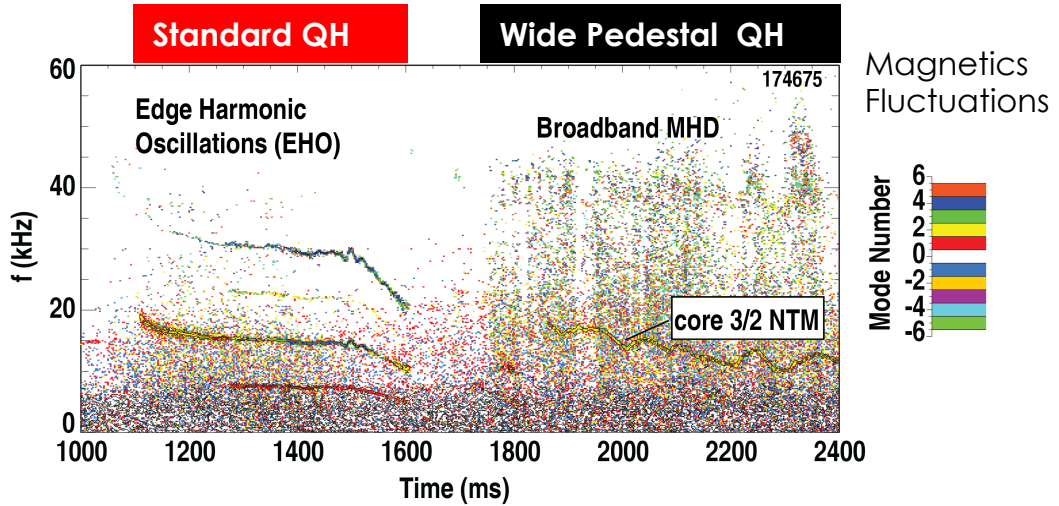

[1]Burrell et al., Phys. Plasmas (2016)
[2]Chen et al., Nucl. Fusion (2017)
[3]Ernst et al., IAEA EX-2/2 (2018), [4]Burrell et al. (2020)

Wide Pedestal QH-Mode is an example of a Turbulence-Limited Pedestal where *Reduced* Pedestal ExB Shear *Improves* Confinement

- **WPQH-Mode**

$$\nu_{*e}^{ped} = 0.1 - 0.5$$
$$H_{98}^{y2} = 1 - 1.6$$
$$Z_{\text{eff}}^{C} = 2 - 5$$
$$q_{95} = 4.2 - 6$$
$$\mathrm{P_b} = 4 - 7.5\ \mathrm{MW}$$
$$\frac{P_{ECH}}{P_b + P_{ECH}} = 0 - 77\%$$
$$I_p = 0.7 - 1.3\ \mathrm{MA}$$
$$B_t = 2\ \mathrm{T}$$

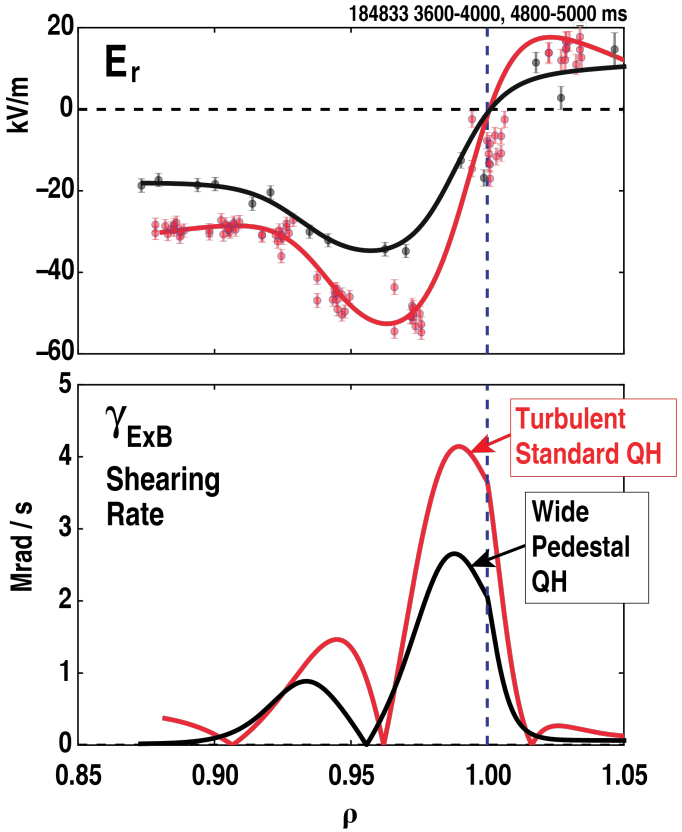

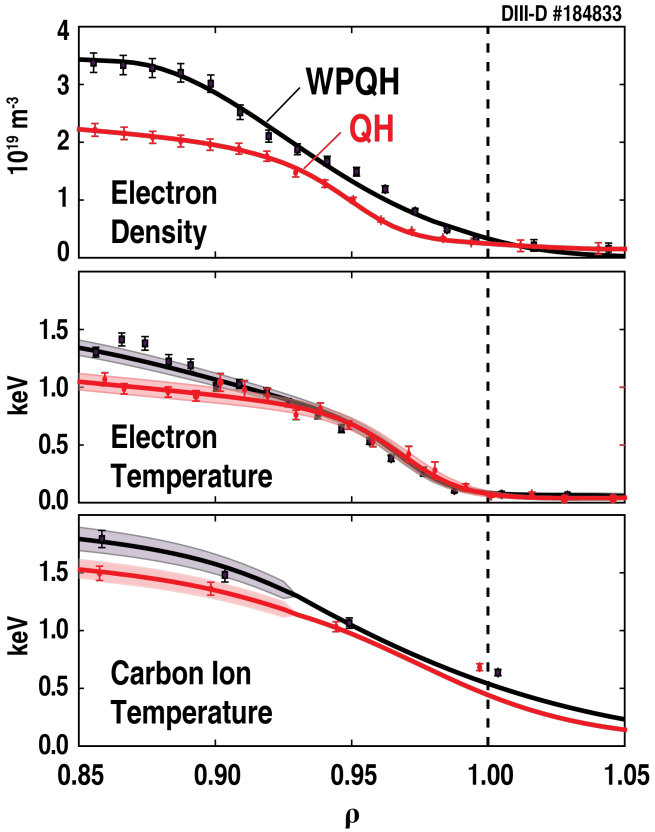

DIII-D NATIONAL FUSION FACILITY

Strike Point Sweeps Past Divertor Probe Arrays Measure Heat Flux Widths, Comparing Wide Pedestal QH and "Turbulent Standard QH-Mode"

- Induce back-transition from Wide Pedestal QH-Mode to Standard QH-Mode ("Turbulent QH") by increasing NBI Torque – intensifying pedestal turbulence
- No coherent MHD activity is observed in either WPQH or Turbulent QH regime

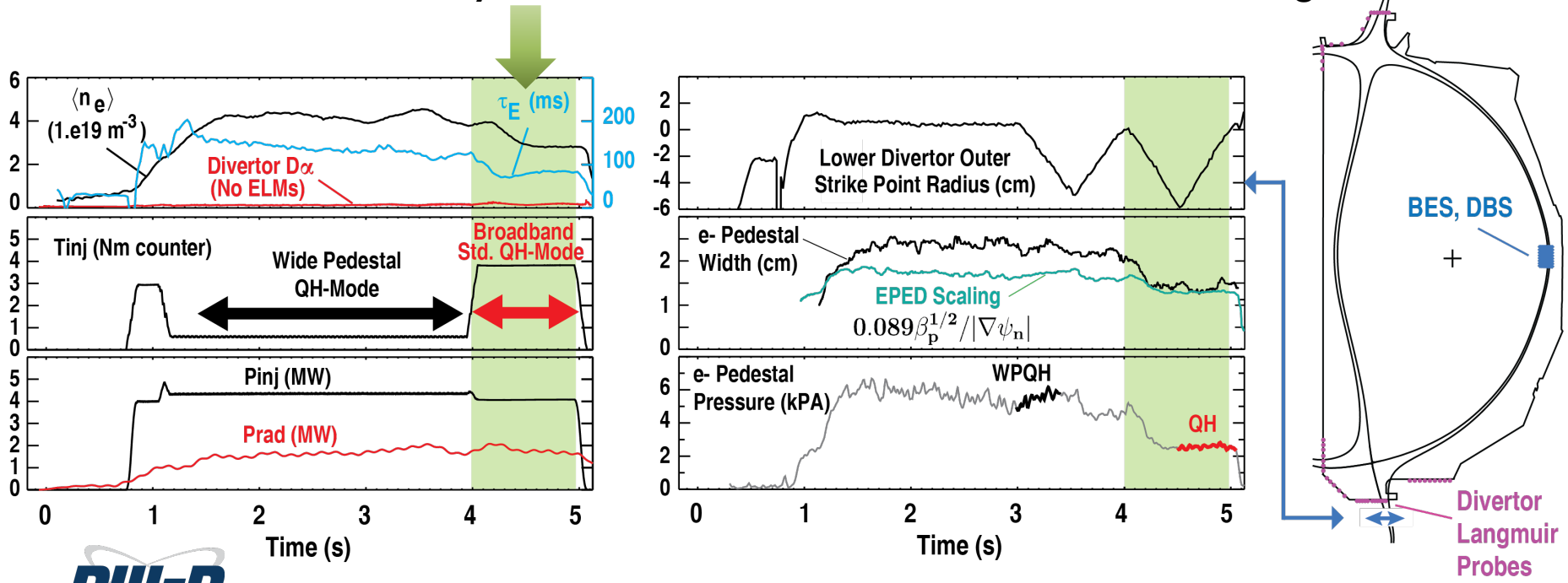

Ernst et al., arXiv (2024), PRL accepted (2024)

Diverter Heat Flux Width Nearly Doubled as Turbulence Intensity Doubles in Transition from WPQH-Mode to Turbulent QH-Mode

- **Measured pedestal electron turbulence intensifies:**
  - Identified as TEM
- **Electron contribution to divertor heat flux doubles profile width λ_q**
  - Similar to ITER predictions [Chang PoP 2017, 2021]

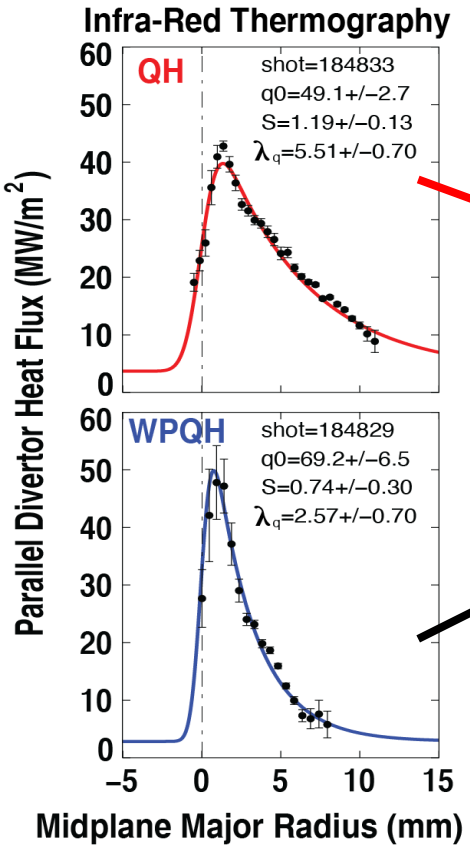

$$\lambda_q^{Goldston} \sim v_{di}\frac{qR}{v_{Ti}} \sim \varepsilon\rho_{pol,i} \propto B_{pol}^{-1}$$

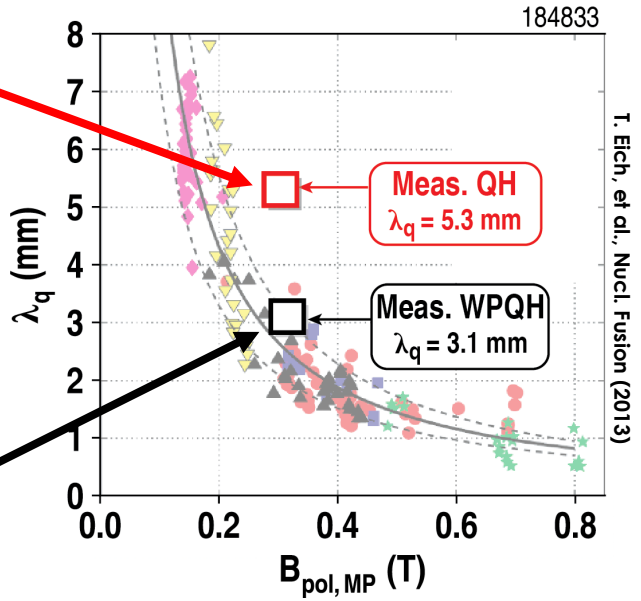

Ernst (MIT), Ku (PPPL), Chang (PPPL), Yan (UW), Bortolon (PPPL), Haskey (PPPL), Laggner (NC State) et al.

Ernst et al., EPS 2023, PRL accepted (2024)

XGC Global Total-*f* EM Simulations with MC Neutrals and Impurities Match Measured Divertor Heat Flux Widths in both WPQH and QH-Mode

- **Measured pedestal electron turbulence intensifies:**
  - Identified as TEM
- **Electron contribution to divertor heat flux doubles profile width λ_q**
  - Similar to ITER predictions [Chang PoP 2017, 2021]

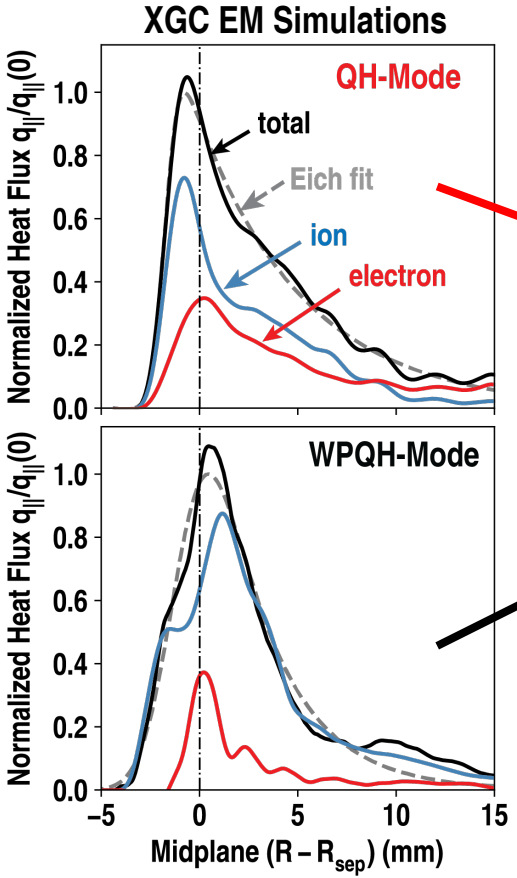

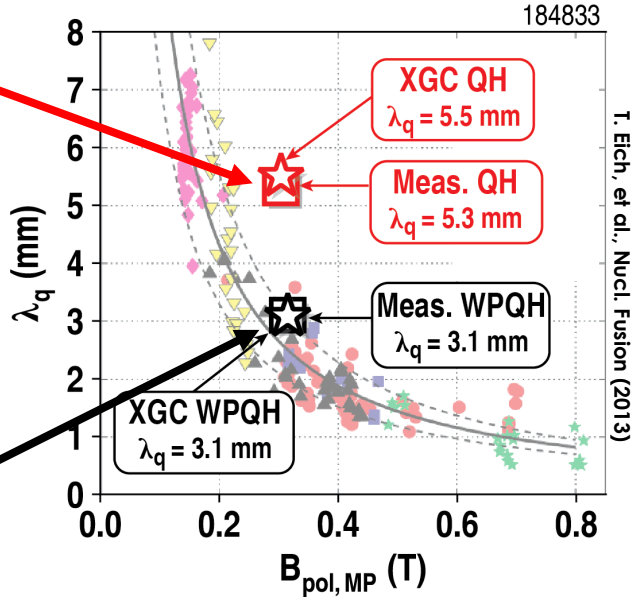

Ernst et al., EPS 2023, PRL accepted (2024)

Ernst (MIT), Ku (PPPL), Chang (PPPL), Yan (UW), Bortolon (PPPL), Haskey (PPPL), Laggner (NC State) et al.

Strong High Frequency Band of Electron Modes Emerges as WPQH ➔ QH

- **Low frequency ion modes show little change in amplitude in WPQH ➔ QH transition**

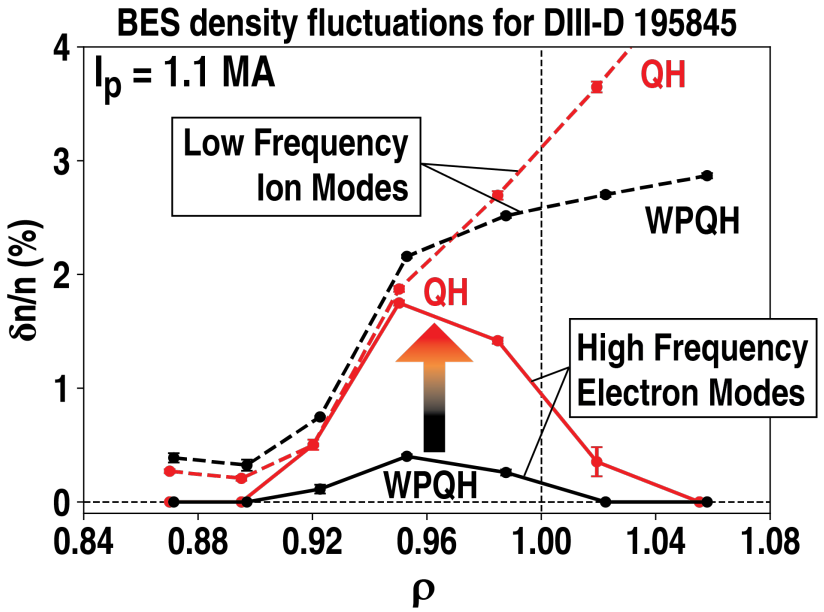

- **Increased $dV_{||}/dr$ due to increased torque during QH can drive TEMs [Ernst PoP 2016]**

BES measurements show pedestal electron feature emerges

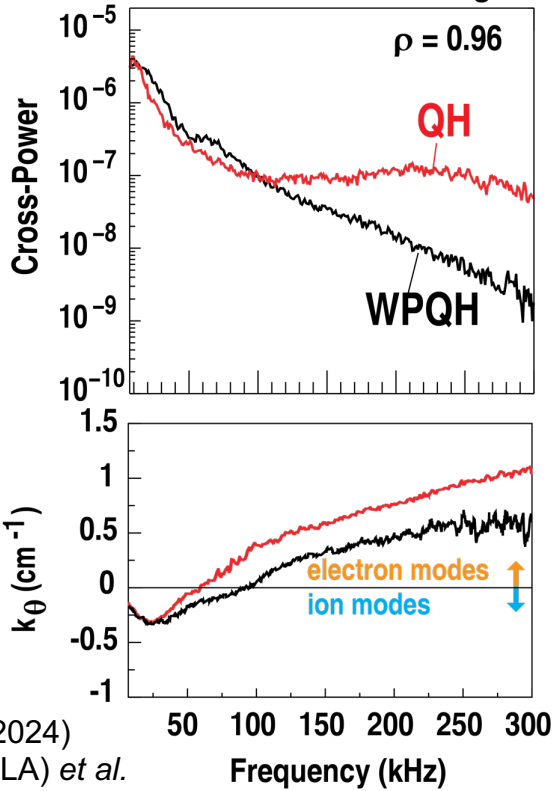

Ernst et al., US TTF Plenary (2022), arXiv (2024) PRL accepted (2024)
Ernst (MIT), Wang (GA), Yan (UW), Khabanov (UW), Rhodes (UCLA) *et al.*

Strong High Frequency Band of Electron Modes Emerges as WPQH ➔ QH

- DBS shows TEM-like fluctuations at shorter wavelengths in QH, consistent with BES
- Magnetic fluctuations from RIP in 100-300 kHz band also double as WPQH ➔ QH

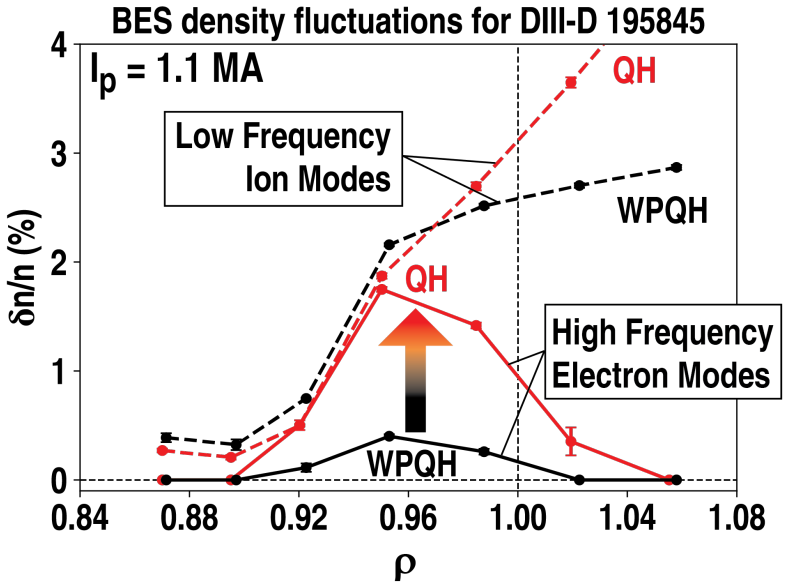

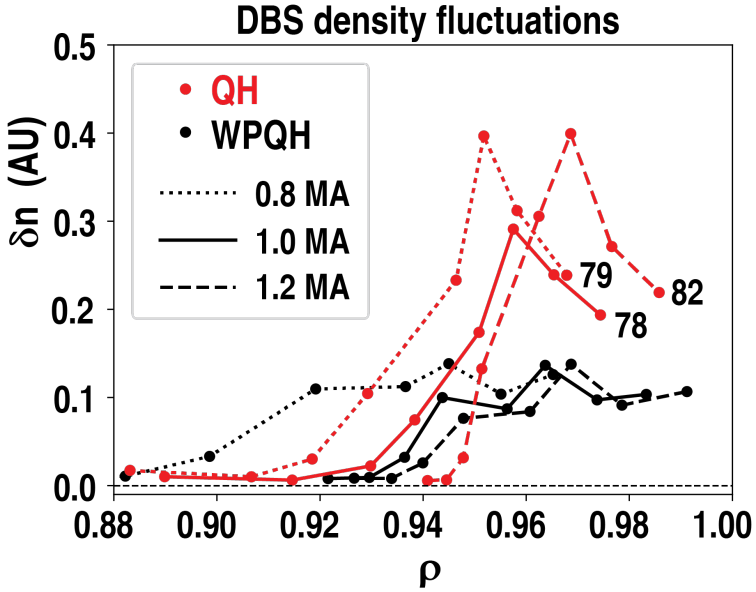

$k_\theta \sim 3 - 5\ \mathrm{cm}^{-1}$

$k_\theta \rho_s \sim 1$

$n \sim 30 - 50$

Global GENE Simulations of a WPQH Mode Discharge Spanning the Full Pedestal Width from n = 10-100 find Pedestal Top TEM

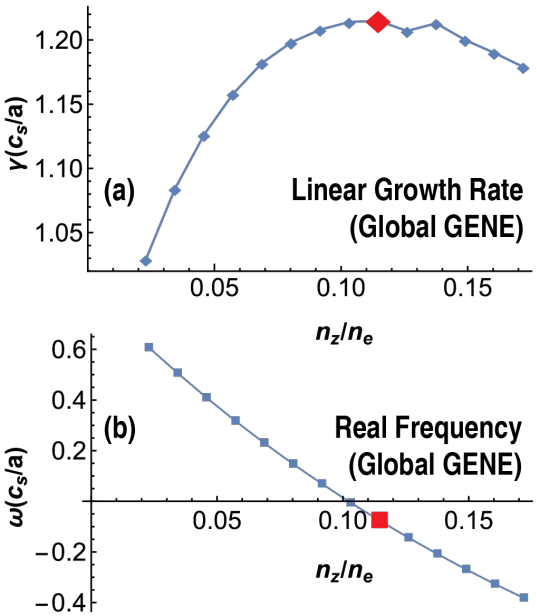

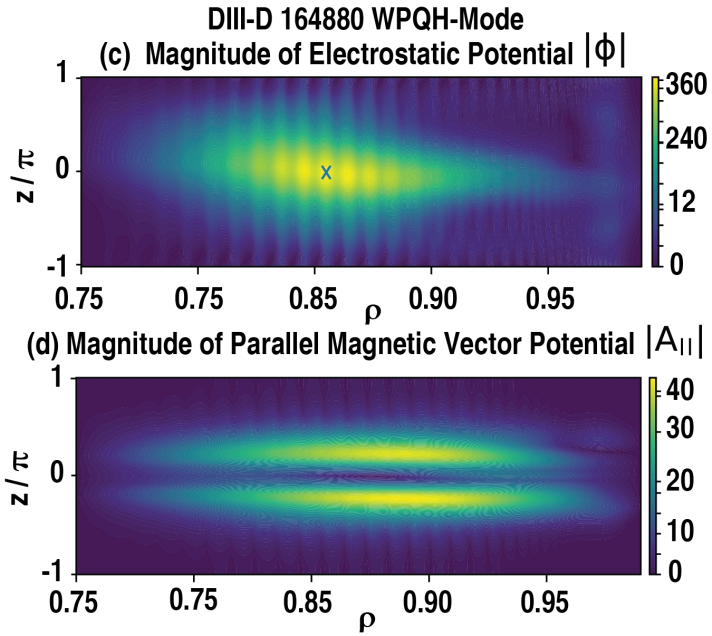

- **Global GENE pedestal simulations of TEM also consistent with improved WPQH confinement with ECH and density pumpout**
- **Separate Nonlinear GENE simulations find ETG turbulence contributes ~1/3 of electron heat flux in pedestal**

- **Fingerprint ratios are consistent with trapped electron mode instabilities. Significant electron heat flux. Dominantly electrostatic.** $\chi_e \gg D_Z > D_e > D_i > \chi_i$

M. Halfmoon (UT-Austin, now DOE), D. Hatch (UT), D. R. Ernst (MIT)

XGC finds increase in electron mode intensity in transition from WPQH to Turbulent QH, with non-adiabatic response

- **Qualitatively consistent with emergence of electron feature in measured fluctuations**

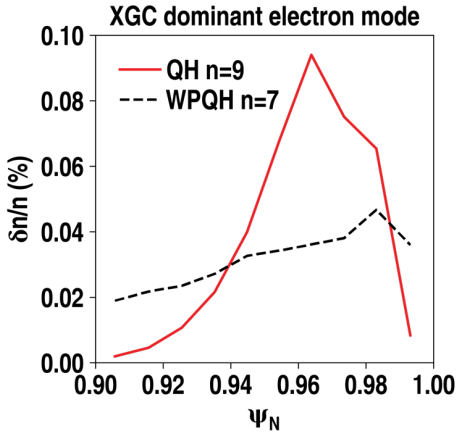

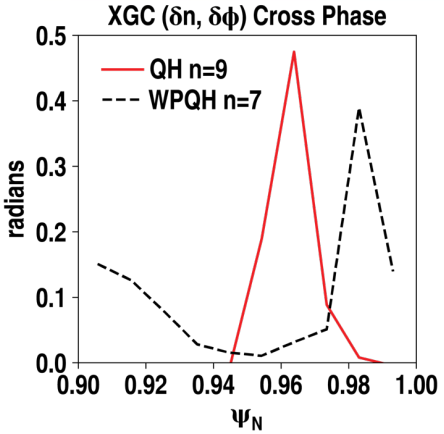

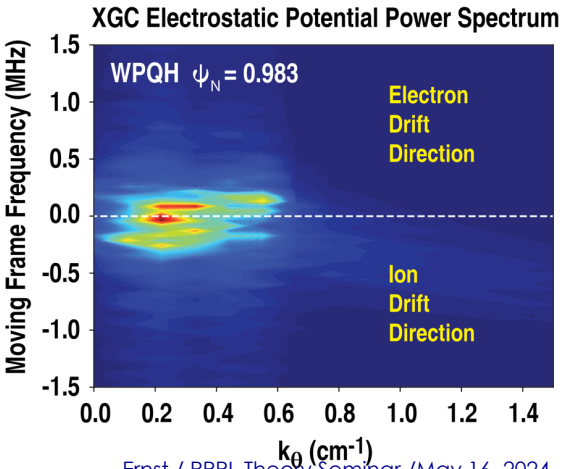

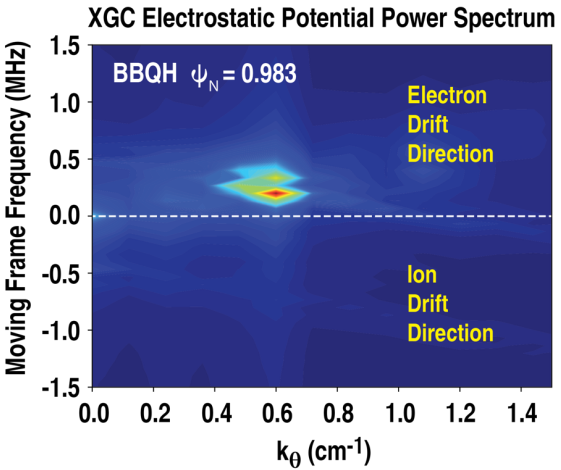

In QH-Mode core, TEM strongly destabilized by sheared parallel flow

- **Nonlinearly, Shear in Parallel Flow Very Important Prior to ECH, but unimportant During ECH as $T_i \rightarrow T_e$**

Prior to ECH (2980 ms)

- **Parallel flow shear lowers TEM critical density gradient: 1.6 ➔ 1.2**

During ECH (3080 ms)

- **Parallel flow shear unimportant (except momentum transport)**

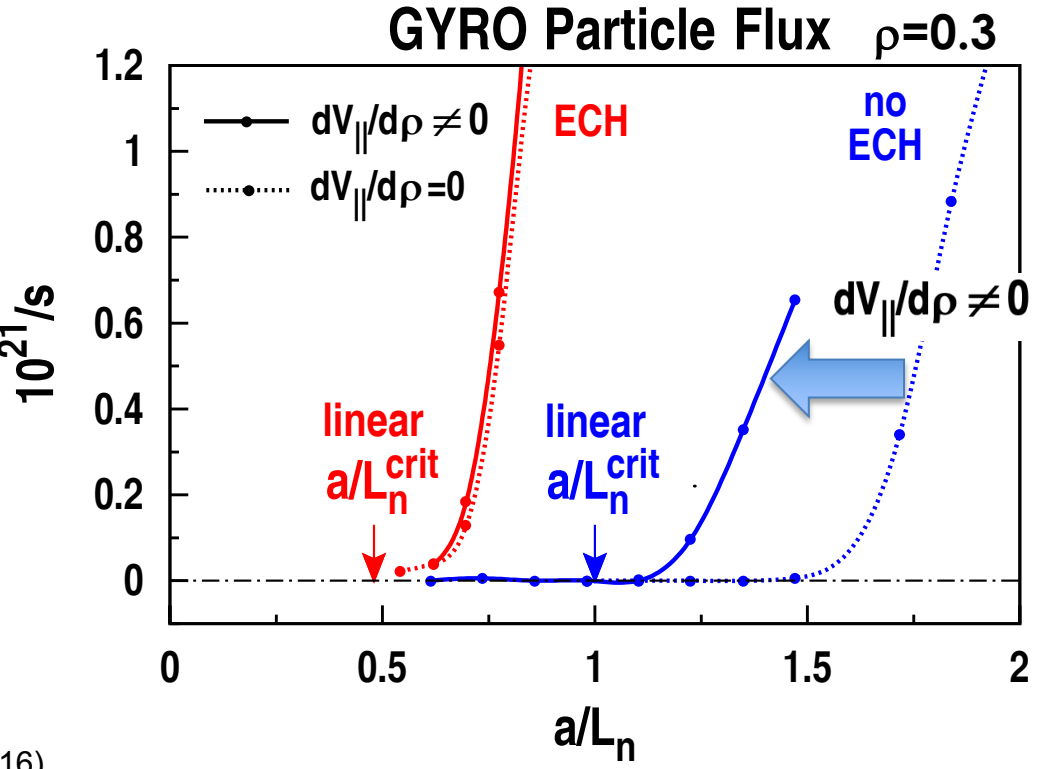

Ernst et al, Phys. Plasmas (2016)

I_p scan shows no simple trend with B_p – does not follow ITPA scaling

- Non-Monotonic trend in λ_q with B_p
- Re-organizes as monotonically increasing trend with $\tilde{n}/n$

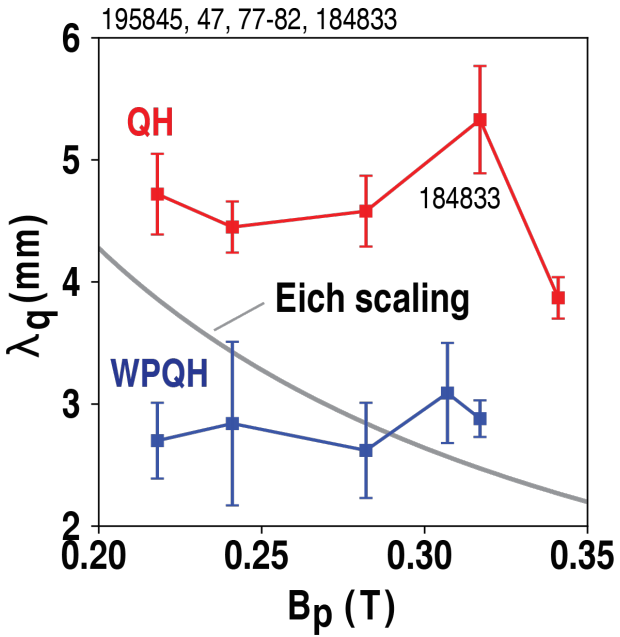

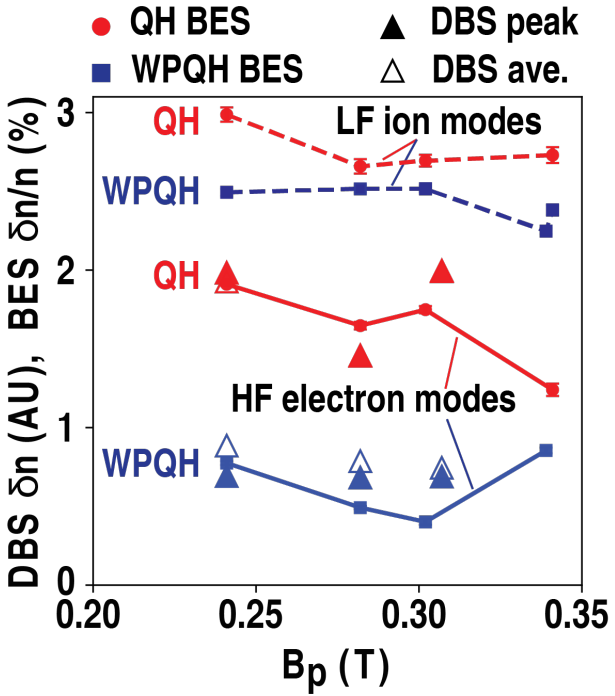

Turbulence Broadening of Divertor Heat Flux Width λ_q Demonstrated in Turbulence Limited QH-Mode Pedestals using Direct Measurements

Eich function fitted to divertor Langmuir probe $q_{||}$ profiles [T. Eich NF 2013]

$$q_{||}(\bar{s}) = \frac{q_0}{2}\exp\left[\left(\frac{S}{2\lambda_q}\right)^2 - \frac{\bar{s}}{\lambda_q f_x}\right]\mathrm{erfc}\left(\frac{S}{2\lambda_q} - \frac{\bar{s}}{S f_x}\right) + q_{\mathrm{BG}}$$

$$\bar{s} = s - s_0 = (R_{\mathrm{mid}} - R_{\mathrm{sep}})f_x$$

$f_x = 5.3$ **flux area expansion factor**

$$\lambda_{\mathrm{int}} = \frac{\int [q_{||}(s) - q_{\mathrm{BG}}]ds}{q_{||0}} \approx \lambda_q + 1.64\,S$$

Integral heat flux width at divertor

- **Both λ_q and S increase with $\tilde{n}/n$**
- **I_p scan shows no trend with B_p – does not follow ITPA scaling**

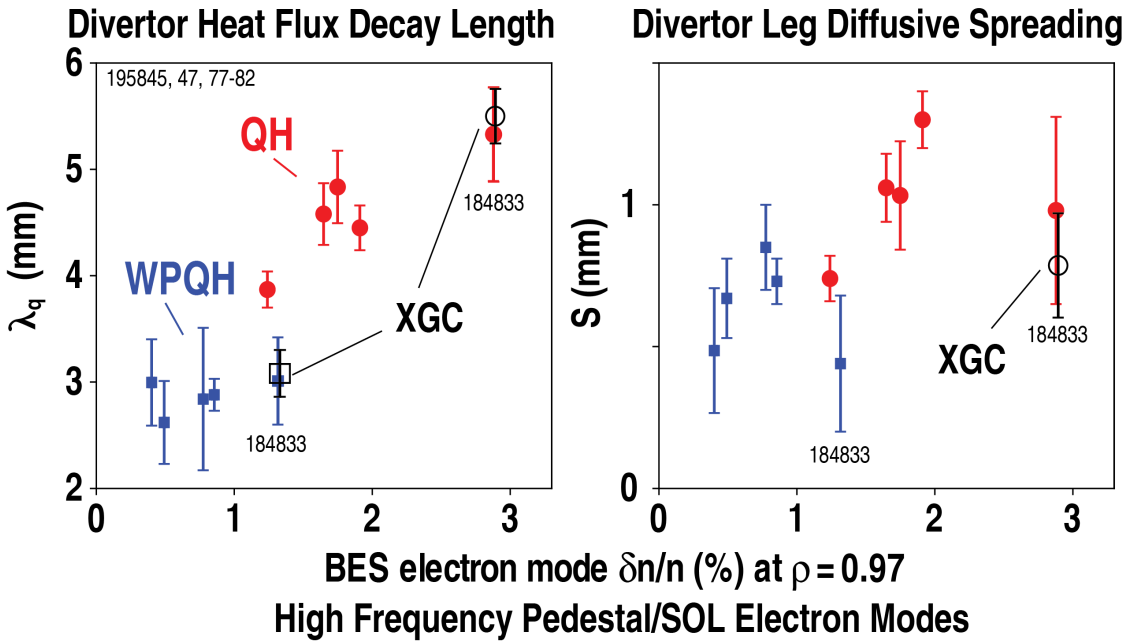

Ernst et al., arXiv (2024), PRL accepted (2024).

DIII-D NATIONAL FUSION FACILITY

Langmuir Probe and Infrared Thermography in Agreement

- **Langmuir probe analysis assumed standard sheath heat transmission coefficient** [Stangeby 2000]

$$\gamma = q_{se}/(T_e\Gamma_e) \approx 7$$

$$q_{se} = (\gamma_e + \gamma_i)T_e\Gamma_e$$

$$\gamma_e = 2 + |eV_{sf}|/T_e + |eV_{\mathrm{pre-sheath}}|/T_e$$
$$= 2 + 3 + 1/2 = 5.5$$
$$\gamma_i \approx 2$$

- ***This assumes no radial transport or drift out of flux tube…etc.***
- ***But λ_q is independent of γ, so LP still provide direct evidence of broadening***

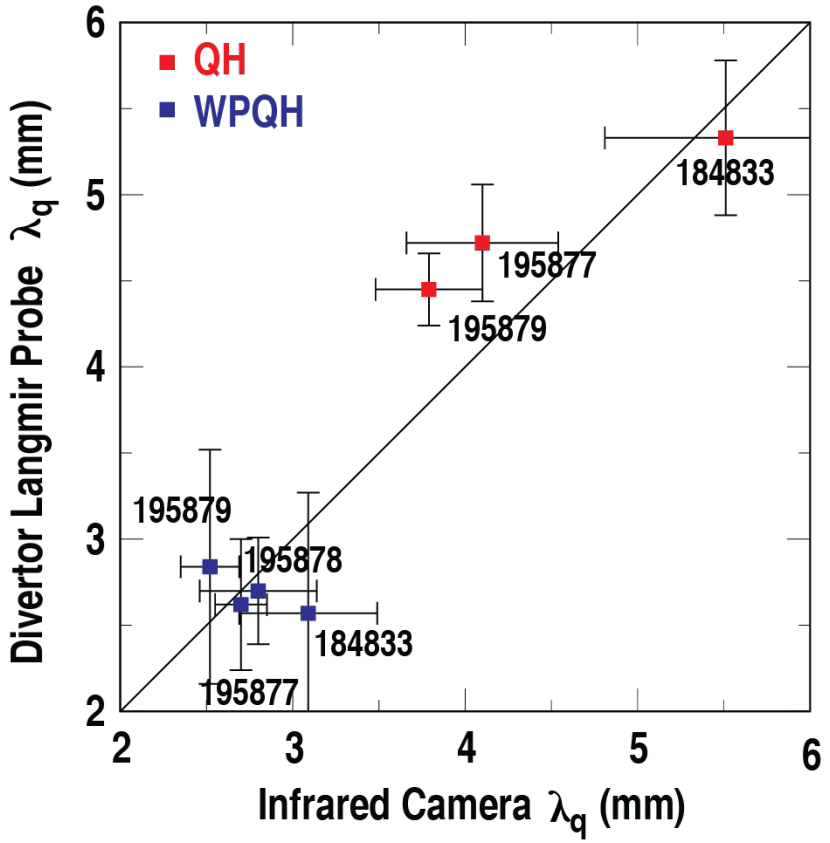

Infra-red Thermography matches Langmuir Probes where available

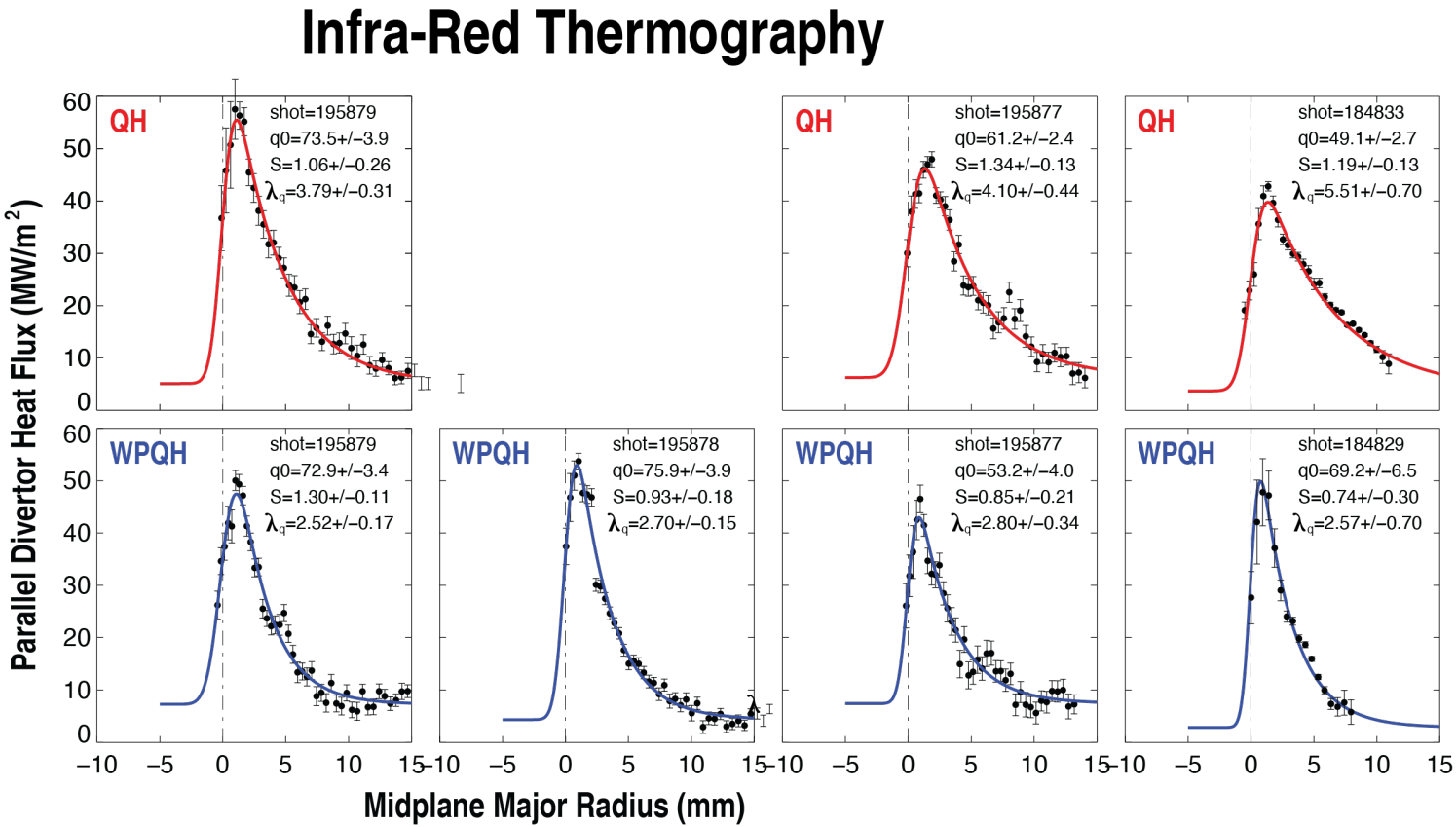

Langmuir Probe Measured Heat Flux Profiles ($\gamma_{SH} = 7$) and Eich Fits

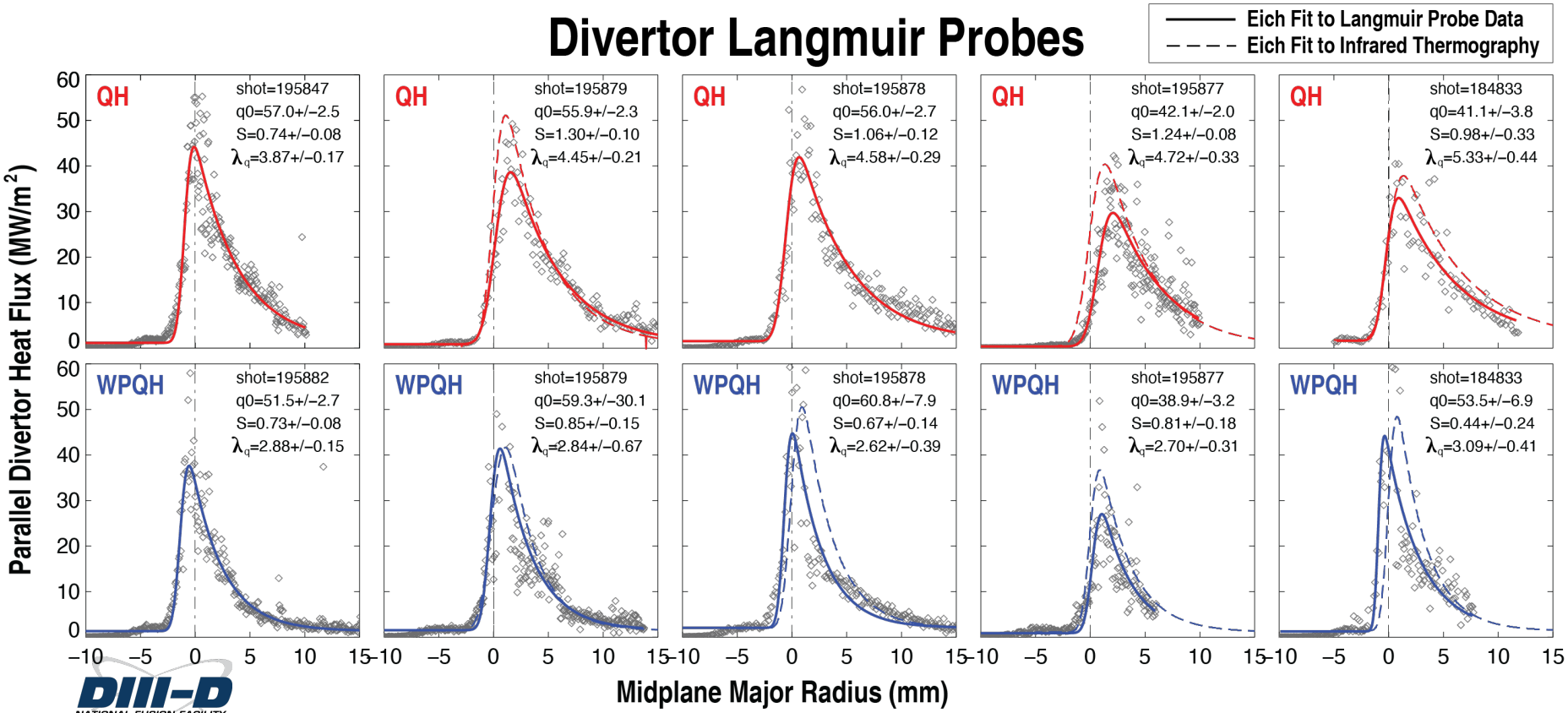

Predicted ExB Shear Suppression of Pedestal Turbulent Transport is Much Weaker at Small ρ_* in Future Machines: Naturally non-ELMing?

- **Ratio of shearing rate to drift wave growth rate in pedestal of fixed width Δ scales[1,2] with ρ_*, also increasing radial correlation lengths[3]**

$$en_iE_r \simeq \frac{dp_i}{dr} \sim \frac{p_i}{\Delta}; \qquad \gamma_{\rm lin} \sim \frac{v_{Ti}}{\Delta}; \qquad \gamma_{\rm E\times B} \simeq \frac{1}{B}\frac{dE_r}{dr}; \qquad \boxed{\frac{\gamma_{\rm E\times B}}{\gamma_{\rm lin}} \sim \frac{\rho_i}{\Delta} \sim \frac{a}{\Delta}\rho_*}$$

- **From theory[4] and global pedestal gyrokinetic simulations,[5] transport reduction due to ExB shear scales asymptotically as[2]**

$$\frac{Q}{Q_{\rm GB}} \sim \left(\frac{\gamma_{E\times B}}{\gamma_{\rm lin}}\right)^{-2} \sim \left(\frac{\Delta}{a}\right)^2 \frac{1}{\rho_*^2} \sim \frac{\beta_p^{2\alpha_1}}{\rho_*^2}$$

Larger turbulent fluxes at smaller ρ_* and higher β_p

KBM (EPED): $\Delta \sim \beta_p^{\alpha_1}$ $\qquad \alpha_1 \sim 0.5 - 0.75$

- **This *suggests* pedestal turbulence *may* be sufficient to maintain ELM stability below the peeling-ballooning boundary[6]**

[1]Kotschenreuther et al. IAEA v1. p.371 (1996).
[2]Kotschenreuther et al. Nucl. Fusion 57, 64001 (2017).
[3]Chang et al., Phys. Plasmas 28, 022501 (2021).
[4]Zhang and Mahajan Phys. Fluids B 4, 1385 (1992).
[5]Hatch et al., Plasma Phys. Control. Fusion 60, 084003 (2018).
[6]Ernst IAEA 2018 EX/2-2 also APS DPP (2022).

Summary/Conclusions

- **High-performance, Intrinsically non-ELMing H-Mode regimes *may naturally arise* in future machines due the scaling of ExB shear with ρ_* and transport with $1/\rho_*^2$**
- **Intrinsically Non-ELMing regimes bring new benefits:**
  - No ELMs to erode/melt divertor (unacceptable in future machines)
  - Turbulence limited pedestal exhibits broadened divertor heat flux widths
  - Turbulence shown to double divertor heat flux width, reducing peak heat load, matched by XGC
  - Broadening is due to TEM turbulence in pedestal, *similar to ITER predictions* [Chang 2017, 2021]
    - Electron channel contribution to divertor heat flux emerges to broaden heat flux profile
  - Results supported by direct measurements of total (IR) and electron (LP) divertor heat flux profiles
  - Given fixed profiles and physical sources, XGC quantitatively reproduces results
    - XGC exhibits very similar fluctuation signatures to experiment, without adjustments to profiles

D. R. Ernst, A. Bortolon, C. S. Chang, S. Ku et al., Phys. Rev. Lett. (2024)
accepted for publication. https://arxiv.org/abs/2403.00185

References

K. H. Burrell et al., Phys. Plasmas **8**, 2153 (2001).
A. M. Garofalo et al., Phys. Plasmas **22**, 056116 (2015).
K. H. Burrell et al., Nucl. Fusion **60**, 086005 (2020).
X. Chen et al., Nucl. Fusion **60**, 092006 (2020).
D. R. Ernst et al., in Proc. 27th IAEA FEC (2018), IAEA-CN-258/EX/2-2.
S. Houshmandyar et al., Nucl. Fusion **62** 056024 (2022).
D. R. Ernst, A. Bortolon, C. S. Chang, S. Ku et al., Phys. Rev. Lett. (2024) accepted for publication. https://arxiv.org/abs/2403.00185 (see references therein)
C. S. Chang et al., Phys. Plasmas **28**, 022501 (2021).

D. R. Ernst et al., "New Developments in Wide Pedestal QH-Mode Transport from Core to SOL," Plenary Talk, 2022 US-EU Transport Task Force Meeting, Santa Rosa, California April 5-8, 2022.

G. Yu et al., "ECEI characterization of pedestal fluctuations in Quiescent H-mode plasmas on DIII-D," Plasma Phys. Contr. Fusion (2022).

D. R. Ernst et al., "Results of the 2022 U.S. Joint Research Target on Intrinsically Non-ELMing Enhanced Confinement Regimes,"
EPS invited (2023), APS invited (2023).

Acknowledgement

We thank Morgan Shafer (Oak Ridge National Laboratory) and Tom Osborne (General Atomics) for extensive comments and efforts during the DIII-D internal review process; as well as both Referees for their detailed and useful constructive comments. We would like to acknowledge Keith Burrell (General Atomics), Florian Effenberg (Princeton Plasma Physics Laboratory), Qiming Hu (Princeton Plasma Physics Laboratory), Al Hyatt (General Atomics), Zeyu Li (General Atomics), Adam McClean (Princeton Plasma Physics Laboratory), Tomas Odstrcil (General Atomics), Theresa Wilks (Massachusetts Institute of Technology), Guanying Yu (Univ. California, Davis), and Lei Zeng (Univ. California Los Angeles) for contributions to the experiments featured.

This material is based upon work supported by the U.S. Department of Energy, Office of Science, Office of Fusion Energy Sciences, using the DIII-D National Fusion Facility, a DOE Office of Science user facility, under Award(s) DE-FC02-04ER54698, DE-SC0014264, DE-AC02-09CH11466, DE-SC0019004, DE-AC52-07NA27344, DE-NA0003525, DE-FG02-08ER54999, and DE-SC0019352. This research used resources of the National Energy Research Scientific Computing Center (NERSC), a U.S. Department of Energy Office of Science User Facility located at Lawrence Berkeley National Laboratory, operated under Contract No. DE-AC02-05CH11231. This research used resources, via the INCITE program, of the Oak Ridge Leadership Computing Facility at the Oak Ridge National Laboratory, which is supported by the Office of Science of the U.S. Department of Energy under Contract No. DE-AC05-00OR22725.